International Journal of Advanced Astronomy, 14 (2) (2026) 30-48

International Journal of Advanced Astronomy

Website: www.sciencepubco.com/index.php/IJAA
https://doi.org/10.14419/0q2t9v67
Research paper

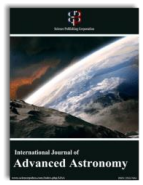

Time-Dependent Radiation–Matter Interactions in Young Stellar Systems: Variability, Circumstellar Response, Observational Diagnostics, and Radiative-Transfer Modelling

Ranjith R *

Department of Physics and Research centre, Nesamony Memorial Christian College, Marthandam, Kanyakumari 629 165, Tamil Nadu, India
**Corresponding author E-mail: ranjithmsuphysics.research@gmail.com*

Received: 29-08-2026, Accepted: 23-09-2026, Published: 29-09-2026

Abstract

Young stellar objects exhibit variability over timescales ranging from minutes to years due to the combined influence of stellar activity, ac-cretion, circumstellar extinction, dust evolution, and structural changes in protoplanetary disks. These processes modify the radiation field and alter the thermal, dynamical, and observational properties of the surrounding gas and dust. Many studies examine individual mecha-nisms separately, yet the observed variability commonly arises from the interaction of multiple processes operating simultaneously. This review examines young stellar systems as coupled radiation–matter environments in which changes in the central source propagate through circumstellar material and generate wavelength-dependent observational signatures. The fundamental radiative processes governing absorp-tion, scattering, thermal re-emission, dust sublimation, radiative equilibrium, and time-dependent response are discussed together with their effects on photometric, spectroscopic, infrared, and polarimetric observations. Observational diagnostics are linked to physical parameters such as optical depth, dust temperature, grain properties, disk geometry, and accretion activity. Radiative-transfer approaches, including one-dimensional, multidimensional, Monte Carlo, thermo-chemical, and time-dependent models, are critically compared in terms of physical assumptions, predictive capability, and limitations. A source–response–observable framework is proposed to connect variable radiation fields with circumstellar evolution and measurable quantities. The review identifies current challenges associated with parameter degeneracy, simplified geometries, and non-equilibrium processes, and outlines future directions combining coordinated multiwavelength observations with time-dependent radiative-transfer modelling.

Keywords: *Young Stellar Systems; Radiation–Matter Interaction; Circumstellar Dust; Stellar Variability; Radiative Transfer; Time-Domain Astronomy.*

1. Introduction

Radiation emerging from a young stellar system does not propagate through a static environment. Accretion flows, circumstellar disks, dusty envelopes, stellar activity, and evolving dust structures continuously modify the radiation field and its interaction with surrounding matter. Young stellar objects (YSOs), including T Tauri and Herbig Ae/Be systems, can exhibit variability over a wide range of temporal scales as a consequence of stellar activity, rotational modulation, accretion variability, variable extinction, scattering, and changes in disk structure [1–4]. Herbig Ae/Be stars are particularly useful intermediate-mass pre-main-sequence systems for studying the connection between stellar accretion, circumstellar gas and dust, and disk evolution [5].

Radiative transfer provides the physical basis for describing this coupling. Absorption, emission, and scattering by gas and dust redistribute radiation across wavelength and direction, while the thermal response of circumstellar material determines how changes in the incident radiation field appear at later times. A variation in stellar or accretion luminosity can heat nearby dust, modify the dust sublimation boundary, change the amount of radiation intercepted by the disk, and alter the infrared emission received by an observer [7]. The response is controlled by optical depth, dust opacity, grain properties, density, disk geometry, and viewing angle [6–8]. Recent work on dust evolution also shows that grain growth, radial transport, settling, and substructure can substantially modify the physical properties of circumstellar disks and their observable emission [8].

Young stellar systems are particularly useful for studying these processes because several variable components coexist within the same environment. Optical and ultraviolet emission can respond directly to changes in the stellar or accretion source, while infrared emission traces the thermal response of circumstellar dust. Spectral lines provide information about the gas component and its velocity structure, whereas polarization constrains the contribution and geometry of scattered radiation [3], [9], [10]. Multi-epoch spectroscopy of 38 Herbig Ae/Be stars, based on 337 optical spectra, found variability in several circumstellar emission lines; He I 5876 equivalent-width changes

Copyright © Ranjith R. This is an open access article distributed under the Creative Commons Attribution License, which permits unrestricted use, distribution, and reproduction in any medium, provided the original work is properly cited.

exceeded one order of magnitude in some cases and Hα changes reached a factor of about four, showing that gas diagnostics can vary on observable timescales and need not respond identically [9].

The same photometric change can have different physical origins. Optical fading may result from variable extinction rather than a decrease in intrinsic luminosity, while optical brightening may arise from increased accretion, stellar activity, or a reduction in circumstellar obscuration. UX Ori-type systems provide a clear example of this degeneracy: brightness variations can reach several magnitudes, while simultaneous colour and polarization changes provide evidence for the role of circumstellar scattering and obscuration [10], [11].

Observational studies have established that variability extends across several temporal regimes. Recent TESS observations of 188 intermediate-mass young stars found that approximately 95% of the Herbig Ae/Be stars in the sample were variable over timescales from about 10 min to 1 month, with stochastic variability being the most common morphology [4]. Spectroscopic monitoring has also shown that circumstellar emission lines can vary over timescales ranging from hours to months [9]. These observations indicate that the variable radiation field and the circumstellar response should be studied as a coupled temporal system rather than as independent observational phenomena.

Radiative-transfer modelling has provided an important theoretical framework for connecting these observations with physical conditions. One-dimensional and two-dimensional models are useful for calculating radial temperature structures, spectral-energy distributions, and simplified disk configurations, while three-dimensional Monte Carlo approaches can incorporate asymmetric geometries, scattering, thermal emission, and polarization. Time-dependent approaches extend this framework by following the response of circumstellar material to a changing radiation field [6], [12]. A recent three-dimensional time-dependent Monte Carlo implementation, for example, was developed to calculate temperature distributions, images, spectral-energy distributions, scattered radiation, and thermal re-emission from variable sources embedded in dust distributions such as circumstellar disks and shells [12].

Radiative-transfer modelling must also account for the evolving nature of dust. Dust growth, radial drift, settling, fragmentation, and the formation of symmetric and asymmetric substructures affect both the physical structure and radiation-processing properties of disks [8]. The increasing availability of high-resolution observations from facilities such as ALMA and SPHERE has made these structures directly accessible, but the physical conditions in optically thick regions remain difficult to constrain [8]. A central problem in the existing literature is that variability mechanisms are often investigated separately. Studies of accretion variability, stellar activity, UXOR-type extinction, dust evolution, or disk structure provide detailed information on individual processes, but the observational signatures of these mechanisms can overlap. Accretion itself also remains physically differentiated across the stellar-mass range. For Herbig Ae/Be stars, published accretion-rate measurements indicate a change in the mass dependence near $4\dot{M}$, with magnetospheric accretion favoured for later-type Herbig stars while the accretion mechanism of earlier-type Herbig Be stars remains less certain [5], [13]. A second gap concerns the temporal connection between the variable source and the circumstellar response. A change in the incident radiation field does not necessarily produce an instantaneous change in the observed infrared or scattered emission. Light-travel time, dust heating and cooling, sublimation, condensation, optical-depth changes, and dynamical rearrangement can introduce different response timescales. Time-dependent radiative-transfer calculations provide a means of explicitly treating these effects and of connecting variable illumination with evolving scattered and thermal emission [12].

A third problem is parameter degeneracy. Similar optical light curves can be produced by different combinations of intrinsic luminosity variation, accretion rate, dust optical depth, scattering geometry, and disk inclination. A single observable such as Δm cannot uniquely identify the physical mechanism. Stronger constraints can be obtained by combining brightness variation with colour, emission-line equivalent width, infrared flux, polarization degree, polarization position angle, and temporal lag [9–11]. This creates a need for a review framework that connects each observable to the physical parameter it can constrain. A further limitation is the separation between simplified model geometries and the asymmetric structures expected in real circumstellar environments. Warps, clumps, gaps, non-uniform dust distributions, and evolving inner rims can modify the observed radiation field. Recent disk studies show that both symmetric and asymmetric substructures are widespread, while the physical properties of dust in optically thick regions remain incompletely constrained [8], [14].

The scientific motivation of this review is closely related to the observational study of variable stars and circumstellar matter, including the UX Ori phenomenon, where coordinated photometric and polarimetric observations established the importance of circumstellar scattering and obscuration [10], [11]. Modern time-domain surveys, multiwavelength facilities, spectropolarimetric observations, and time-dependent radiative-transfer calculations now provide an opportunity to extend this physical interpretation from individual variability phenomena towards a more integrated description of evolving star–disk environments [4], [12], [15].

This review addresses that gap by treating young stellar systems as time-dependent radiation–matter systems in which the variable source and circumstellar response are physically coupled. The review first establishes the radiative processes controlling absorption, scattering, thermal re-emission, radiative equilibrium, and dust sublimation. It then synthesizes the principal mechanisms responsible for variability, including accretion, stellar activity, variable extinction, dust evolution, and disk-structure changes, using characteristic timescales, amplitudes, wavelength dependence, and observational signatures as comparison criteria. Building on this perspective, the present review extends the discussion toward a time-dependent framework that links variable radiation, circumstellar response, multiwavelength observables, and radiative-transfer modelling [6], [20], [37]. The observational section connects optical photometry, spectroscopy, infrared measurements, ultraviolet and X-ray observations, and polarimetry with the physical quantities that can be inferred from them. Radiative-transfer approaches are then compared according to geometry, temporal treatment, predicted observables, and computational limitations.

The major contribution of this review is the development of a common source–response–observable framework:

Variable radiation source → Radiation--matter interaction → Circumstellar response → Multiwavelength observables → Physical parameter inference

Within this framework, observable quantities such as photometric amplitude Δm, colour variation, emission-line equivalent width EW, polarization P, infrared flux variation, and temporal lag Δt are linked to physical parameters including optical depth, dust temperature, dust distribution, disk geometry, inner-rim location, and accretion activity. The review also identifies where current models remain limited by simplified geometries, fixed dust properties, steady-state assumptions, incomplete gas–dust coupling, and parameter degeneracy. Rather than treating increasing model complexity as an objective by itself, emphasis is placed on models that generate predictions testable through coordinated observations.

The review therefore moves beyond a catalogue of variability mechanisms and observational techniques. Its central objective is to establish how changes in the radiation source propagate through an evolving circumstellar environment and how that response can be recovered from time-dependent, multiwavelength observations. Future progress will depend on combining three-dimensional time-dependent radiative-transfer calculations with coordinated photometric, spectroscopic, infrared, high-energy, and polarimetric observations. Such an

approach can convert observed variability from a phenomenological signal into a quantitative probe of the physical conditions and evolution of young stellar systems.

2. Time-Dependent Radiative Processes in Circumstellar Environments

The radiation field in a young stellar system is controlled by the luminosity and spectral characteristics of the central source together with the density, composition, geometry, and optical properties of the surrounding material. Accretion episodes, stellar activity, changes in the inner disk, and variations in the dust distribution can alter the radiation received by different regions of the circumstellar environment. The resulting response is not determined by the incident radiation alone. The optical depth, grain properties, local thermal conditions, and spatial distribution of the material influence how rapidly the radiation is absorbed, scattered, re-emitted, or transmitted [16], [17].
Radiative transfer provides the basic framework for describing this interaction [16], [19]. For a ray travelling through circumstellar material, the specific intensity changes according to

$$\frac{dI_\nu}{ds} = -\alpha_\nu I_\nu + j_\nu \tag{1}$$

where I_ν is the specific intensity, α_ν is the absorption coefficient, and j_ν represents emission. This expression describes the balance between attenuation of radiation and local emission. In a variable young stellar system, both terms can change with position and time because the radiation source and the circumstellar material are not necessarily stationary [23], [30].
For a time-dependent radiation field, the transfer equation must retain the explicit temporal derivative. In the observer-frame formulation, the monochromatic specific intensity satisfies

$$(1a)\ (1/c)\ \partial I\nu(r,n,t)/\partial t + n \cdot \nabla I\nu(r,n,t) = -\chi\nu\, I\nu(r,n,t) + j\nu(r,n,t) \tag{2}$$

where $\chi\nu$ is the extinction coefficient and $j\nu$ is the emissivity. The steady equation used above is recovered when $\partial I\nu/\partial t = 0$. The explicit time term is important when the variability timescale of the illuminating source is comparable to the light-crossing time of the circumstellar region or to the local material-response time.

For an extended disk, the radiation incident on a point r at time t is also retarded. A source variation emitted at t' contributes at a location r' at approximately $t = t' + |r - r'|/c$. Thus the local radiation field can be represented schematically as $J\nu(r,t) = J\nu[r, L\nu(t-\tau)]$ with τ including the relevant propagation path. This retardation term produces wavelength-dependent lags when different bands originate in spatially extended regions.

The optical depth,

$$\tau_\nu = \int \alpha_\nu \, ds \tag{3}$$

provides a useful measure of the interaction between radiation and matter. Small optical depths allow a substantial fraction of the incident radiation to pass through the material, while large optical depths produce stronger attenuation and increase the role of reprocessing within the circumstellar environment [16], [19]. Changes in optical depth can alter the observed intensity even when the intrinsic luminosity of the central source remains unchanged. This point is important for young stellar objects because variations in the observed light curve can arise from either intrinsic change in the source or changes in the material located along the line of sight [20].
The interpretation of optical depth also depends on wavelength. Dust opacity varies across the electromagnetic spectrum, so the same circumstellar structure can appear optically thick in one wavelength range and comparatively transparent in another [16], [17]. A change in the dust column can consequently produce different amplitudes and temporal behaviour at optical, near-infrared, and longer infrared wavelengths. Multiwavelength observations are useful in this situation because the wavelength dependence of the response provides information about the location and properties of the absorbing and emitting material.

2.1. Absorption and thermal re-emission by circumstellar dust

Dust grains play a central role in the conversion of stellar and accretion radiation into infrared emission. Absorbed radiation increases the grain temperature, and the stored energy is subsequently released through thermal emission [16], [18]. The dust temperature is controlled by the incident radiation field, grain absorption properties, grain size distribution, and the local geometry of the disk or envelope [17].
For a variable radiation source, the dust temperature cannot always be treated as a fixed equilibrium quantity. An increase in stellar or accretion luminosity changes the energy received by the dust and can shift the local thermal balance. The infrared response then depends on both the change in the radiation field and the thermal response of the dust [22], [23]. A similar process occurs when the incident luminosity decreases, with the observed infrared emission responding to the subsequent cooling of the circumstellar material.
A non-equilibrium treatment can be expressed through the grain energy equation

$$(2a)\ C_d(T_d)dT\ d/dt = 4\pi \int k_{abs},\nu\, [J\nu(r,t) - B\nu(T_d)]\, d\nu + \Gamma_{gd} - \Lambda_{gd} \tag{4}$$

where C_d is the grain heat capacity, k_{abs},ν is the absorption opacity, and $g\Gamma_{gd}$, Λ_{gd} represent gas-to-dust heating and cooling terms when gas–dust thermal coupling is relevant. This formulation makes clear that dust temperature does not necessarily follow the instantaneous radiative-equilibrium value. The characteristic response depends on grain heat capacity, opacity, local radiation density, and gas coupling. This creates an important distinction between source variability and observed infrared variability. An optical increase does not necessarily produce an instantaneous or proportional infrared increase. The response depends on the distance between the radiation source and the emitting dust, the optical depth of the intervening material, and the thermal properties of the grains [23]. The time delay between different wavelength bands can thus contain information about the spatial distribution of the circumstellar material.
Dust re-emission also modifies the energy distribution emerging from the system. Radiation absorbed at shorter wavelengths can appear as enhanced infrared emission after reprocessing by the dust. The observed spectral energy distribution is consequently linked to both the

incident radiation and the distribution of dust capable of absorbing and re-emitting that radiation [17], [18]. This connection makes infrared variability a useful probe of changes in the inner and outer regions of circumstellar disks.

2.2. Scattering and wavelength-dependent radiation redistribution

Scattering provides another pathway through which circumstellar material modifies the observed radiation [20], [24]. The scattered component depends on grain size, wavelength, albedo, scattering phase function, viewing angle, and the spatial distribution of dust [25],[27]. The observed flux can contain both direct radiation from the central source and radiation redirected by circumstellar grains. The relative contribution of these components changes with the geometry of the system. In a nearly face-on disk, the direct stellar component can dominate the observed signal, while systems viewed at higher inclination can be more strongly affected by obscuration and scattered light. Small changes in the position or density of circumstellar dust can then produce changes in both brightness and polarization [25], [26].
Scattering is particularly relevant when photometric variations are interpreted as changes in intrinsic stellar luminosity. A decrease in direct radiation caused by obscuration can be accompanied by an increased relative contribution from scattered light. The resulting colour and polarization behaviour may differ from a simple reduction in intrinsic luminosity [20]. Photometry alone can thus leave an ambiguity that can be reduced through simultaneous polarimetric and spectroscopic observations [25-27]. Figure 1 summarizes the physical framework connecting variable stellar or accretion radiation with its interaction with circumstellar gas and dust through absorption, scattering, and thermal re-emission, ultimately determining the radiation received by an observer.

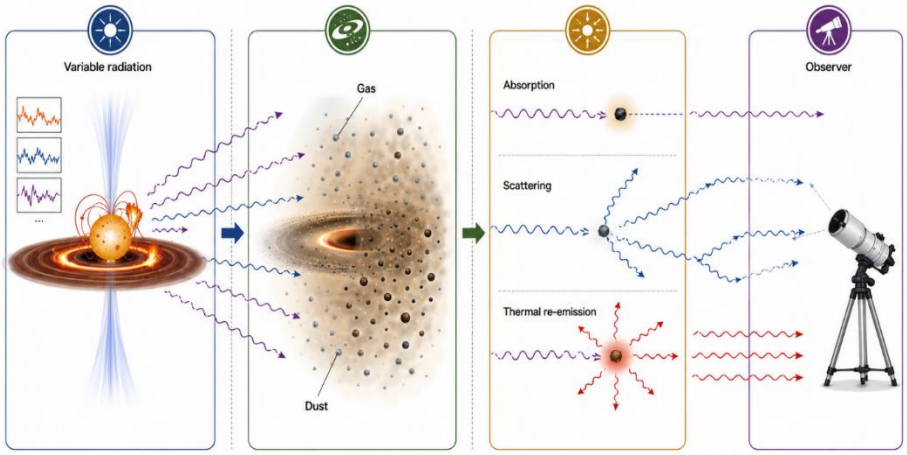

Fig. 1: Schematic Representation of Time-Dependent Radiation–Matter Interaction in A Young Stellar System, Showing Variable Stellar/Accretion Radiation, Circumstellar Dust and Gas, Absorption, Scattering, Thermal Re-Emission, and the Resulting Radiation Received by an Observer.

2.3. Dust sublimation and inner-disk response

The inner region of a circumstellar disk is strongly influenced by the thermal stability of dust. When the local radiation field raises the grain temperature towards the sublimation regime, dust can be removed from the hottest region and the effective inner boundary of the dust-rich disk can move outward. [18], [21], [22] A reduction in luminosity can permit dust to survive or reform closer to the central source, depending on the local density, grain properties, and thermal history. The commonly adopted dust sublimation temperature lies near 1600–1800 K for several relevant grain compositions, but the exact value is not universal. Grain composition, size, pressure, surface properties, and the local radiation environment influence the temperature at which sublimation becomes important. [21], [22] Treating Tsub as a single fixed value can consequently simplify the physical description of the inner disk.
The adopted 1600–1800 K range should be regarded as representative rather than universal. Sublimation temperatures depend on grain composition, size and surface properties: carbon-rich/graphitic grains can survive at higher temperatures than many silicate grains, for which values around 1000–1500 K are often adopted in disk models. The sublimation rate also depends on local gas pressure or density because the equilibrium between evaporation and re-condensation is pressure dependent. Consequently, the sublimation front should be treated as a material- and environment-dependent boundary rather than a single fixed temperature [21, 22, 83].
The movement of the inner dust boundary has observational consequences. A change in the inner-rim location modifies the amount of stellar radiation intercepted by the disk and changes the near-infrared emission produced by hot dust. [18], [21] The response can also affect the illumination of regions farther from the inner rim. The observed infrared variation is thus connected not only to dust temperature but also to changes in disk geometry. [28] This coupling is important in variable young stellar systems. A luminosity change can modify the dust temperature, the sublimation boundary, and the illumination pattern. The altered dust distribution then changes the radiation field reaching other parts of the disk. The radiation field and circumstellar structure are consequently linked through a feedback process rather than behaving as independent components. [21], [22]

2.4. Time-dependent response of circumstellar material

The response of circumstellar matter to a variable radiation field occurs over several physical timescales. Radiation propagation, dust heating and cooling, gas thermal adjustment, recombination, and dynamical rearrangement need not occur over the same interval. [23,30] The observed variability can consequently contain delayed responses from different regions of the system. For rapid changes in the central radiation source, the light-travel time establishes the first temporal scale. The thermal response of dust introduces another timescale, while changes in disk structure operate on longer dynamical timescales. [22], [23] When the source varies faster than the material can adjust, the circumstellar environment can depart from instantaneous radiative equilibrium.
This distinction affects the interpretation of multiwavelength light curves. A short optical event may be followed by a delayed infrared response if the observed infrared emission originates from dust located farther from the central source. The measured delay is influenced by the physical distance, dust temperature, optical depth, and thermal response. [23] It should not be interpreted as a direct distance measurement without accounting for these effects. Non-equilibrium behaviour can also occur in the gas component. Changes in the radiation

field can modify ionization and heating; while cooling and recombination may require additional time. In regions where these processes are slow compared with the variability of the radiation source, steady-state calculations may not capture the temporal evolution of the emitting material. [23]

2.5. Coupled radiation–matter response

The processes discussed above are connected through a common physical chain:

Variable radiation source → absorption/scattering → thermal and ionization response → dust and gas evolution → modified radiation field → observed variability

This chain shows why the observed signal cannot always be assigned directly to a change in stellar luminosity. The radiation received by an observer contains contributions from the central source, circumstellar absorption, scattered radiation, thermal re-emission, and changes in disk geometry. [16], [20]
The coupling becomes more complex when several processes operate at the same time. Accretion variability can increase the radiation field, dust can respond through heating and sublimation, and the resulting change in dust distribution can modify the radiation reaching other parts of the disk. [18], [22] Stellar activity can add short-duration ultraviolet and X-ray variations to the same system. A single observed light curve can consequently contain contributions from processes operating on different spatial and temporal scales. [23] This is one reason why time-dependent radiative-transfer models are useful for young stellar systems. A steady-state model can provide the temperature and radiation structure for a selected configuration, but it does not directly describe how that structure evolves following a change in the radiation source. [19], [23] Time-dependent calculations can follow the propagation of the radiation change and the subsequent thermal response of the circumstellar material. [30] Table 1 summarizes the principal radiative processes, their governing quantities, quantitative descriptors, and expected observational consequences. The table is retained because it provides a compact comparison of the physical mechanisms discussed throughout this section.

Table 1: Major Radiative Processes Governing Radiation–Matter Interaction in Circumstellar Environments

Process	Governing quantity	Quantitative descriptor	Observable consequence	Relevance to YSOs	Reference
Absorption	τ_λ	$I_\lambda = I_{\lambda,0}e^{-\tau_\lambda}$	Flux attenuation	Variable extinction	[16, 18]
Scattering	Albedo ω_λ	$0 \le \omega_\lambda \le 1$	Scattered flux, polarization	UXOR variability	[20, 25]
Thermal re-emission	T_d	$F_\lambda \propto B_\lambda(T_d)$	IR excess/variability	Heated circumstellar dust	[19, 23]
Dust sublimation	T_{sub}	$T_{sub} \sim 1600 - 1800$ K	Inner-rim movement	Variable IR emission	[21, 22]
Radiative equilibrium	T_d (r)	$T_d \propto r^{-q}$	Radial temperature structure	Disk emission	[18, 19]
Polarized scattering	P	$P = \sqrt{Q^2 + U^2}\,/\,I$	Polarization variability	Dust geometry	[20, 25]

2.6. Critical synthesis

The literature on circumstellar radiation–matter interaction establishes a clear connection between changes in the radiation source and changes in the surrounding dust and gas. The main physical processes are well defined, but their observational signatures can overlap. Absorption can produce dimming, scattering can alter both flux and polarization, dust heating can increase infrared emission, and changes in disk geometry can modify the radiation reaching the observer [16], [20], [21]. The main difficulty lies in separating these processes when they occur together. A change in optical brightness does not by itself identify whether the source luminosity, accretion rate, extinction, scattering geometry, or dust distribution has changed [20], [25]. The problem becomes harder when the characteristic response times of the different components are comparable. [22], [23]
Current modelling approaches also involve a balance between physical detail and computational cost. Simplified geometries are useful for identifying basic radiative trends, but they cannot represent all forms of disk asymmetry, clumping, warping, or evolving dust distributions. [18], [28] Time-dependent three-dimensional calculations can address a larger part of this parameter space, but they require more computational resources and better constraints on the physical properties of the circumstellar material. [19], [23], [30]. A useful direction for future work is the integration of time-domain observations with radiative-transfer models that evolve the radiation field, dust temperature, optical depth, and disk geometry together. Such an approach can use changes in brightness, colour, infrared emission, spectral features, and polarization as complementary constraints rather than treating each observable independently. [20], [25], [30]
The central point from this synthesis is that variability in young stellar systems is not simply a record of changing stellar luminosity. It is the observable response of a coupled radiation–matter system. [23], [30] This provides the physical basis for examining the specific variability mechanisms and their characteristic observational signatures in the next section.

3. Radiation-Driven Variability in Young Stellar Systems

Variability in young stellar systems can arise from changes in the central star, accretion flow, or circumstellar material [31], [32], [41]. These mechanisms operate over different spatial and temporal scales and can produce overlapping photometric, spectroscopic, infrared, and polarimetric signatures [31], [32]. The observed light curve is therefore a combined response of the stellar source and its circumstellar environment rather than a direct measurement of a single physical process.
The distinction between variability mechanisms requires consideration of amplitude, duration, wavelength dependence, recurrence, and changes in spectral or polarization properties [31], [32], [37]. Multi-epoch observations provide evidence that the circumstellar environment can change on timescales ranging from hours to months [9], [41]. For example, a multi-epoch study of 38 Herbig Ae/Be stars based on 337 optical spectra found measurable variability in the major circumstellar emission lines, with Hα equivalent-width changes reaching a factor of about four and He I 5876 changes exceeding one order of magnitude in individual objects [9]. Hα line-profile changes were found in about 70% of the sample [9]. These measurements show that variability is not restricted to broadband flux changes and that the gas component can respond on relatively short timescales.

3.1. Accretion-related variability

Accretion is one of the main sources of luminosity variability in young stellar systems [33], [34]. Material moving from the circumstellar disk towards the central star releases gravitational energy, producing excess emission that can contribute to the optical and ultraviolet radiation field [33]. Changes in the mass-accretion rate can alter both the luminosity of the accretion region and the radiation incident on the inner disk [32–34]. The observational response depends on the magnitude and duration of the change in accretion rate [32–34]. A short accretion fluctuation can produce a temporary increase in optical or ultraviolet emission, while a longer episode can modify the thermal structure of the inner disk and increase infrared emission from heated dust [32], [33]. The response is not expected to be identical at all wavelengths because the stellar/accretion emission and the reprocessed dust emission originate from different regions [32].

Spectroscopic measurements provide an additional way to identify accretion variability [9], [33]. Hα is widely used as an indicator of circumstellar gas activity, but its variability does not map directly onto a single accretion parameter [9]. In the 38-star multi-epoch study, the typical relative variability of Hα equivalent width was about 0.19 using the mean definition reported by the authors, while individual objects showed changes up to a factor of about four [9]. The Hα width at 10% of the peak intensity showed a lower typical relative variability of about 0.09, and changes by a factor of about 2.5 were observed in some objects [9]. These measurements are useful for interpreting the physical origin of line variability [9]. Equivalent width measures the line relative to the local continuum, while line flux is affected by both the emitting gas and the stellar continuum. A change in equivalent width can therefore result from a change in circumstellar emission, continuum variability, or both. Simultaneous photometry and spectroscopy provide a better way to separate these contributions [9], [33].

The relationship between different emission lines also places limits on a single-process interpretation [9]. Hα and [O I] 6300 Å variability was correlated for many objects in the multi-epoch sample, while the different lines showed different levels of relative variability. The He I and Na I D lines were among the more variable features, whereas [O I] and Hα showed lower relative changes in the same dataset [9]. The different response of these lines suggests that gas located in regions with different excitation, density, and velocity conditions contributes to the observed variability.

3.2. Stellar activity and flares

Magnetic activity produces variability on shorter timescales than many accretion and disk-evolution processes [35], [36]. Flares can produce rapid increases in ultraviolet, optical, and X-ray emission followed by a decline as the active region cools [35], [36]. The effect on circumstellar material depends on the energy released, duration of the event, and distance from the central source. Rotational modulation produces a different temporal pattern. Starspots or other non-uniform surface regions can cause periodic changes as the star rotates [25], [41]. The observed amplitude depends on spot coverage, temperature contrast, stellar inclination, and the distribution of active regions. Periodic signals can therefore provide information about stellar surface structure, but the presence of a circumstellar disk can introduce additional periodic or quasi-periodic signals [25], [31].

Time-domain photometry provides a quantitative view of the range of these behaviours. A study of young stellar objects in the Pelican Nebula reported optical fading and brightening events reaching about two magnitudes in some pre-main-sequence stars [25]. Nearly 30% of the variables showed strong periodic signatures attributed to cold-spot modulation, while accretion bursts and extinction events had average optical amplitudes above one magnitude [25].

More recent TESS observations extend the time-domain coverage to much shorter sampling intervals. A study of 188 intermediate-mass young stars found that about 95% of the Herbig Ae/Be stars in the sample were variable over timescales from approximately 10 minutes to one month, with stochastic variability being the most common light-curve morphology [36]. This result places short-timescale variability within a much broader observational context than individual ground-based monitoring campaigns.

The presence of variability alone does not identify magnetic activity [35], [36]. Rapid changes accompanied by ultraviolet or X-ray enhancement provide stronger evidence for energetic stellar events, while periodic optical modulation can support a rotational origin [25], [35]. Simultaneous observations at multiple wavelengths are needed when short-duration stellar activity overlaps with circumstellar variability [31], [32].

3.3. Variable extinction by circumstellar material

Observed dimming in a young stellar system can result from a reduction in intrinsic luminosity or from an increase in the optical depth of material along the line of sight [18], [20], [31]. Circumstellar dust can produce the latter through clumps, filaments, warped disk regions, or other non-uniform structures [18], [37]. The wavelength dependence of extinction provides a useful diagnostic [20], [37]. If the dimming is caused by dust absorption, the shorter-wavelength flux is generally affected more strongly than the longer-wavelength flux. The resulting colour change can be combined with polarization measurements to distinguish extinction-related events from intrinsic luminosity changes [20], [37].

The amplitude of extinction events can also be large enough to overlap with accretion-driven variability. The Pelican Nebula study reported optical fading and brightening events of up to about two magnitudes in several pre-main-sequence stars, while accretion bursts and extinction events had average amplitudes above one magnitude [25]. This overlap shows why amplitude alone is not sufficient to identify the mechanism [25], [31]. UXOR-type variability provides a particularly useful example of this problem [20], [37]. A decrease in direct stellar light caused by circumstellar obscuration can increase the fractional contribution of scattered radiation. The system can then become relatively bluer at deep minima and show enhanced polarization [20], [37]. The combination of brightness, colour, and polarization is more informative than the light curve alone.

The geometry of the obscuring material controls the observed behaviour [18], [37]. A compact dust clump crossing the line of sight can produce a short event, while a warped or extended disk structure can generate repeated or longer-duration changes [18], [37]. The duration of the event therefore contains information about both the spatial scale of the obscuring structure and its orbital motion.

3.4. Disk structure and dust evolution

Changes in disk structure modify both the radiation received by the circumstellar material and the radiation that reaches the observer [18], [22], [38], [42]. Variations in the height of the inner disk, dust concentration, inclination, or inner-rim position can alter the projected emitting and absorbing regions [18], [22], [38]. Dust sublimation provides a direct connection between luminosity variability and disk geometry [22]. An increase in luminosity can heat dust close to the sublimation boundary and move the effective dust-rich inner region

outward [22]. A decrease in luminosity can allow dust to survive closer to the central source if the local density and thermal conditions permit it. The infrared response then reflects changes in both dust temperature and emitting area [22], [32].

This process can generate a delayed or non-linear response [22]. A change in the central luminosity first modifies the radiation field. The dust temperature responds to the altered irradiation, and the dust distribution can then evolve if the temperature approaches the sublimation regime. The resulting change in geometry modifies the radiation intercepted by other parts of the disk [22], [38]. Disk structure can also produce variability without a large change in the intrinsic luminosity of the central star [18], [37]. A rotating warp or clump can periodically modify the line-of-sight optical depth, while changes in the inner rim can alter the amount of hot dust visible to the observer [18], [22], [37]. Such effects can generate photometric variability with similar amplitudes to those produced by accretion [31], [32].

The interpretation of disk-driven variability therefore benefits from combining optical and infrared observations [32], [39], [41]. Optical changes can trace extinction or direct stellar emission, whereas near-infrared emission is more sensitive to hot dust near the inner disk [32], [41]. A correlated change in both bands supports a connection between the central radiation field and the inner circumstellar environment, while different amplitudes or time delays can indicate radiative-transfer or geometric effects [32].

3.5. Characteristic timescales

The timescale of variability provides one of the most useful constraints for separating physical mechanisms [31], [40], [41]. The characteristic intervals should be treated as approximate ranges rather than fixed boundaries because the response depends on stellar mass, disk geometry, accretion state, dust properties, and observing wavelength [31], [32]. Stellar flares can evolve over minutes to hours [35], [36]. Rotational modulation generally occurs over hours to days, depending on the stellar rotation period [25], [41]. Accretion variability can persist from days to years [33], [34], while changes in disk structure and dust distribution can extend over months to years or longer [32], [38], [40]. Observational studies support variability across these ranges rather than a single characteristic timescale [31], [40], [41]. The TESS study of intermediate-mass young stars, for example, detected variability from approximately 10 minutes to one month, with stochastic behaviour common among the Herbig Ae/Be sample [36]. The timescale alone does not uniquely identify the mechanism [31], [41]. A short event can originate from stellar activity or a compact circumstellar structure, while longer variations can arise from accretion, extinction, or disk evolution [31], [32], [40]. The diagnostic becomes stronger when timescale is combined with wavelength dependence and spectral or polarimetric behaviour [20], [31], [37]. For example, a rapid optical increase accompanied by enhanced high-energy emission is consistent with stellar activity [35], [36]. A periodic optical signal can point towards rotational modulation [25], [41]. Optical fading accompanied by colour changes and increased polarization favours circumstellar extinction [20], [37]. A longer-lived optical and infrared variation with changes in emission-line strength can indicate changes in accretion or inner-disk structure [32–34], [40]. Figure 2 summarizes the major variability mechanisms in young stellar systems and highlights their characteristic timescales and observational manifestations.

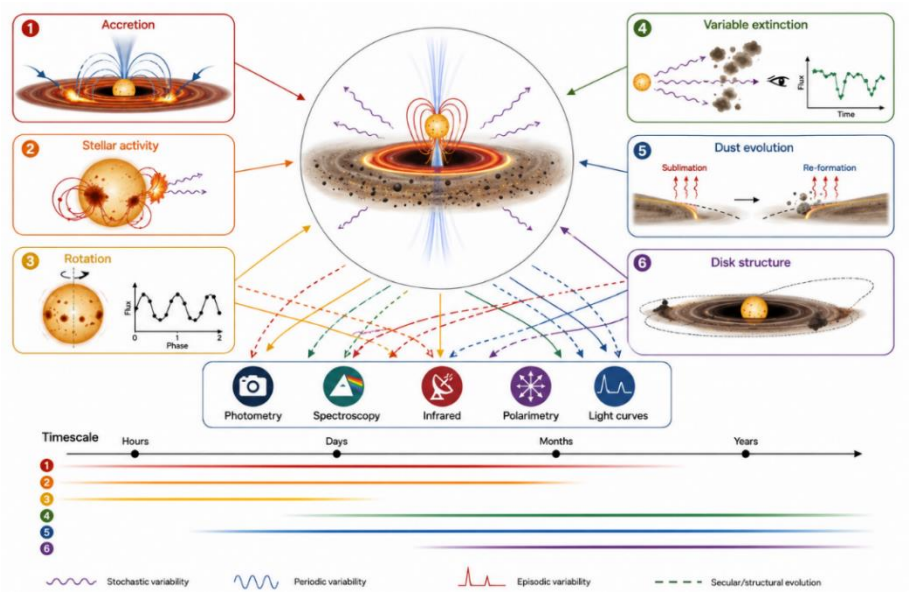

Fig. 2: Major Variability Mechanisms in Young Stellar Systems, Linking Accretion, Stellar, Extinction, Dust, and Circumstellar Structural Processes with Their Characteristic Observational Behaviour.

The principal mechanisms can be compared using four observational dimensions: timescale, amplitude, wavelength dependence, and diagnostic signature. Table 2 retains this comparison and provides a quantitative framework for interpreting the variability discussed in this section.

Table 2: Variability Mechanisms, Characteristic Timescales and Observational Signatures in Young Stellar Systems

Mechanism	Characteristic timescale	Reported amplitude / parameter	Main band	Diagnostic signature	Reference
Stellar flares	minutes–hours	Rapid flux increase	UV/optical/X-ray	Impulsive brightening	[35], [36]
Rotational modulation	hours–days	Typically, sub-mag to multi-mag in active YSOs	Optical/NIR	Periodic variation	[25], [41]
Accretion variability	days–years	Can reach >1 mag; accretion rate can vary strongly	Optical/UV/IR	Continuum + emission-line changes	[31, 33, 34]

Variable extinction	days–weeks	Up to ~ 3 mag in optical	Optical/NIR	Dimming + reddening	[20], [37], [44]
UX Ori eclipses / deep minima	days–months	Typical V-band fading ≈2–4 mag; P ≈5–8%, with >10% reported in deep events	Optical/V band	Dimming, colour reversal (blueing) near deep minima, increased polarization	[20], [37]
Dust sublimation response	hours–days*	$T_{sub} \sim 1600 - 1800$ K	NIR/MIR	Inner-rim/IR changes	[21], [22]
Long-term disk evolution	months–years+	Object dependent	Optical/IR/mm	Long-term SED/flux changes	[32], [39], [40]

*The response timescale depends on local density, grain properties and radiation field.

The UXOR values are particularly useful for our paper because they directly connect the review to Grinin's scientific legacy. Observations and modelling report usual fading depths of about 2–4 mag, with polarization reaching 5–8%, while deeper events can exceed 10% [20], [37].
The coexistence of these mechanisms makes young stellar systems valuable laboratories for studying radiation–matter coupling [31], [32], [40]. Multiwavelength observations are particularly important because different wavelength ranges probe different regions and physical processes [32], [41]. The observational signatures that can be used to separate these mechanisms are discussed in the next section.

3.6. Quantitative separation of accretion and variable extinction

Colour–magnitude trajectories provide a quantitative way to test whether a photometric event is dominated by changing accretion emission, variable extinction, or scattered light. For a band X, mX = −2.5 log10(FX) + CX, so the colour change between two bands is Δ(X−Y) = −2.5 log10[(FX/FY)1/(FX/FY)0]. The slope of a colour–colour trajectory, S = Δ(U−B)/Δ(B−V), can be compared with the expected reddening vector from an adopted extinction law. A trajectory approximately parallel to the reddening vector is consistent with changing line-of-sight extinction, whereas a blue excess produced by a hot accretion component can displace the trajectory away from the pure-extinction locus.
For UX Ori-type events, the observed flux is better represented as a mixture of direct stellar/accretion light, extincted light, and scattered disk light:

$$(3a)\ \mathrm{FX,obs(t)} = [\mathrm{FX,\star} + \mathrm{FX,acc(t)}]\ 10\text{^}(-0.4\ \mathrm{AX(t)}) + \mathrm{FX,sca(t)} \quad (5)$$

At moderate extinction the first term dominates and the source becomes redder as AX increases. At sufficiently deep minima, the extincted direct component becomes small and the relatively less-extincted scattered component becomes an increasing fraction of the observed flux. Because dust-scattered optical light can be comparatively blue, the colour can turn back toward smaller U−B or B−V values while the V-band flux continues to decline; this is the blueing effect. Polarization generally rises at the same stage because the fractional contribution of scattered light increases [20, 37].
The separation is not unique from colour data alone. Accretion brightening should be tested against simultaneous ultraviolet excess and accretion-sensitive emission-line changes, while extinction should be tested against wavelength-dependent dimming and increased polarization. A practical multi-epoch diagnostic is therefore to fit the U−B versus B−V trajectory together with V-band flux, polarization degree P and emission-line equivalent widths. The joint trajectory can be compared with forward radiative-transfer models rather than assigning a mechanism from amplitude alone. Polarized radiative-transfer calculations of UX Ori eclipses show that the colour and polarization response also depends on the geometry and optical depth of the occulting structure [37].

3.7. Critical synthesis

The observational literature supports a multi-process interpretation of variability in young stellar systems [31], [32], [41]. Accretion, stellar activity, extinction, and disk evolution occupy partly different regions of parameter space, but their observational signatures overlap [20], [31], [32]. This overlap is the main reason why a single photometric measurement or a single variability amplitude cannot establish the physical origin of an event. Spectroscopic measurements add information about the circumstellar gas. The multi-epoch study of 38 Herbig Ae/Be stars found variability in several emission lines and showed that the magnitude of variability differs strongly between tracers [9]. Hα changes reached a factor of about four in some objects, while He I 5876 variations exceeded one order of magnitude [9]. The [O I] 6300 Å and Hα variations were correlated for many stars, pointing to a shared contribution from circumstellar gas in those cases [9].
Photometric monitoring adds the temporal information needed to identify recurring or stochastic behaviour [31], [41]. The Pelican Nebula observations found strong periodic signatures in nearly 30% of the variable pre-main-sequence stars, while some accretion and extinction events exceeded one magnitude in optical amplitude [25]. The TESS study extends this picture to minute-to-month timescales and shows that short-timescale variability is common among intermediate-mass young stars [36]. These observations point to a practical diagnostic sequence. Timescale can narrow the range of possible mechanisms, wavelength dependence can indicate whether the variation is dominated by the star or circumstellar dust, spectroscopy can constrain the gas response [9], [33], and polarization can provide information on scattering geometry [20], [37]. None of these observables should be interpreted independently when several mechanisms can operate at the same time [31], [32], [41].
The remaining challenge is to connect observed variability to physical parameters such as mass-accretion rate, dust optical depth, inner-rim radius, grain distribution, and disk geometry [22], [38], [42]. Time-dependent radiative-transfer models provide a route for making this connection. The next section examines how photometric, spectroscopic, infrared, and polarimetric observations can be combined with such models to constrain the physical conditions of young stellar systems.

4. Observational Diagnostics and Theory–Observation Connection

The variable radiation field of a young stellar system leaves signatures across several observational domains. Photometry measures changes in flux and colour, spectroscopy traces variations in gas emission and velocity structure, infrared observations probe thermally emitting dust, and polarimetry provides information on scattering geometry [33], [43]. These measurements do not provide equivalent constraints. Each diagnostic samples a different component of the star–disk environment, and their combination is needed when several physical mechanisms can produce similar light-curve behaviour [49], [50].

4.1. Photometric variability

Time-series photometry provides the basic temporal description of variability through amplitude, duration, recurrence, colour change, and periodicity [40], [44]. A useful measure is the magnitude variation,

$$\Delta m = m_{max} - m_{min,} \tag{3}$$

While the relative flux variation can be expressed as

$$\frac{\Delta F}{F} = \frac{F_{max} - F_{min}}{F_{mx}} \tag{4}$$

These quantities describe the observed change but do not identify its physical origin by themselves. A large Δm can result from intrinsic luminosity changes, accretion activity, or circumstellar obscuration [40]. The temporal pattern and wavelength dependence provide additional constraints.

Multi-band observations are particularly useful for this separation. Extinction generally produces a wavelength-dependent change, while an intrinsic increase in the stellar or accretion luminosity changes the spectral energy distribution in a different way [9], [32]. Simultaneous optical and near-infrared monitoring can therefore test whether the variable component is dominated by the central source or by circumstellar material [48], [50]. The temporal baseline also controls the type of variability that can be identified. Minute-scale monitoring can detect rapid stellar activity, whereas observations extending over months or years are needed to follow accretion changes and disk evolution [32], [40]. A survey of the Pelican Nebula obtained observations over 90 nights and more than 250 epochs, identifying 95 variable stars, including 67 pre-main-sequence variables. Nearly 30% of the variables showed strong periodic signatures [44].

This result illustrates the value of dense temporal sampling. Sparse observations can identify long-term changes but can miss short events or confuse periodic and stochastic variability [40], [44]. For young stellar systems, the sampling interval should therefore be selected according to the physical timescale being investigated.

4.2. Spectroscopic diagnostics

Spectroscopy adds information about the gas that cannot be obtained from broadband photometry. Changes in emission-line equivalent width, line flux, profile shape, asymmetry, and radial velocity can be used to examine accretion flows, winds, and changing line-of-sight conditions [9], [49]. Hydrogen emission lines are commonly used as accretion indicators, but their interpretation depends on both the emitting gas and the continuum against which the line is measured [9].

For a spectral line, the equivalent width can be expressed as [59]

$$EW = \int \left(1 - \frac{F_\lambda}{F_{\lambda,c}} d\lambda\right) \tag{6}$$

Where F_λ is the observed line spectrum and $F_{\lambda,c}$ is the local continuum. A change in EW can occur because the line emission changes, because the continuum changes, or because both change simultaneously. This limits the use of equivalent width as a direct measure of accretion variability [59].

Line-profile information provides an additional constraint. Changes in the velocity distribution can reveal modifications in accretion flows or winds, while asymmetric profiles can indicate that the emitting material is not distributed uniformly [9], [10]. Time-resolved spectroscopy can therefore distinguish changes in total line strength from changes in the velocity structure of the circumstellar gas.

A quantitative example comes from multi-epoch spectroscopy of Herbig Ae/Be stars, where Hα, [O I], He I, and Na I lines showed different levels of variability [9], [58]. This difference is useful because emission lines formed under different physical conditions do not necessarily respond with the same amplitude or timescale. Such behaviour provides evidence that the circumstellar gas cannot always be represented by a single variable component [58].

The strongest interpretation comes from combining line variability with photometry. If an increase in optical brightness occurs together with stronger accretion-sensitive emission lines, a change in the accretion component becomes more plausible. If the continuum changes while the line-emitting region remains comparatively stable, the origin may instead lie in extinction or stellar photospheric variability [48], [49], [56].

4.3. Infrared diagnostics

Infrared observations provide a direct probe of dust that absorbs stellar and accretion radiation and subsequently releases the energy through thermal emission. Near-infrared wavelengths are particularly sensitive to hot dust close to the inner disk, while longer wavelengths sample cooler and more extended material [48], [50].

The observed infrared flux depends on both temperature and emitting area. A simplified representation is [51]

$$F_\lambda \propto A_{em} B_\lambda(T_d) \tag{7}$$

Where A_{em} is the effective emitting area and $B_\lambda(T_d)$ is the Planck function at dust temperature T_d.

This relation is important when interpreting infrared variability. An increase in IR flux does not necessarily mean that the entire dust distribution has become hotter. The emitting area may also change because of inner-rim movement, changes in disk illumination, or dust redistribution [28], [45].
The comparison between optical and infrared light curves provides another quantitative diagnostic. If an infrared variation follows an optical event after a measurable delay Δt, the characteristic light-travel distance can be approximated by [52]

$$R \sim c\,\Delta t \tag{8}$$

provided that the delay is dominated by propagation rather than thermal adjustment. In real circumstellar systems, dust heating and cooling, optical depth, disk geometry, and extended emission regions can all modify the measured delay [52]. The delay should therefore be treated as a constraint on the characteristic emitting region rather than as a direct distance measurement [19], [23].
The combination of near-, mid-, and far-infrared observations can further separate hot inner-disk changes from cooler outer-disk responses. A change concentrated at shorter infrared wavelengths points towards the hot inner dust region, whereas a broader SED change can indicate a larger-scale redistribution of circumstellar material [28], [32], [48].

4.4. Polarization as a geometric diagnostic

Polarization provides information that is difficult to obtain from flux measurements alone. Scattering by circumstellar dust produces polarized radiation, and the polarization degree and position angle depend on the grain properties, scattering geometry, inclination, and distribution of the scattering material [45-47], [53].
The linear polarization degree is given by [53]

$$P = \sqrt{Q^2 + U^2} \,/\, I \tag{9}$$

Where I, Q and U are the Stokes parameters.
A change in P accompanying a photometric variation can indicate a change in the relative contributions of direct and scattered radiation. This is particularly useful during extinction events. When direct stellar light is reduced, the fractional contribution from scattered light can increase, producing a rise in polarization even when the absolute scattered flux changes only modestly [45], [46]. The position angle provides an additional geometric constraint. A stable position angle with changing polarization degree can indicate a change in the relative direct/scattered flux, whereas a changing position angle can indicate a change in the orientation or dominant location of the scattering region [53], [54].
For this reason, polarimetry can help distinguish between intrinsic luminosity variations and circumstellar obscuration.
The combination of photometry, spectroscopy, infrared observations, high-energy measurements, and polarimetry provides complementary constraints on the physical conditions and geometry of young stellar systems. These observations can be linked to circumstellar responses and subsequently to physical parameters through an integrated diagnostic framework, as illustrated in Figure 3 [45], [47], [55].

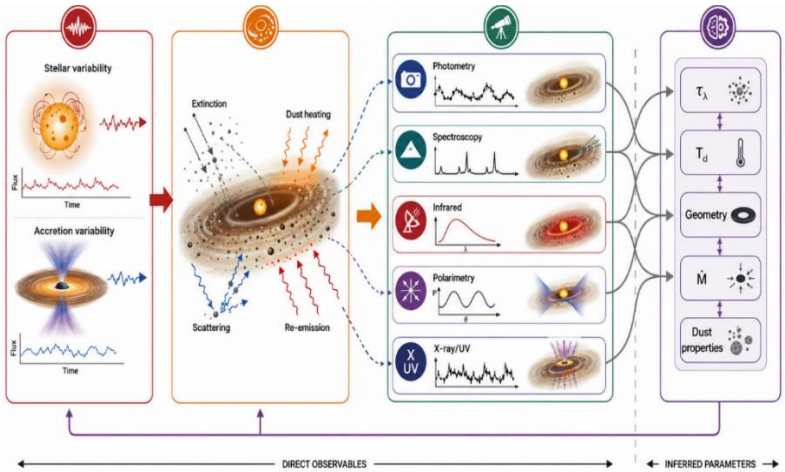

Fig. 3: Connection between Variable Radiation, Circumstellar Response, Observational Diagnostics, and Inferred Physical Parameters in Young Stellar Systems.

The complementary information provided by photometry, spectroscopy, infrared observations, ultraviolet and X-ray measurements, and polarimetry, together with the physical parameters constrained by each diagnostic, is summarized in Table 3.

Table 3: Observational Diagnostics and Physical Parameters Constrained in Young Stellar Systems

Diagnostic	Approx. spectral domain	Temporal information	Primary physical constraint	Quantitative observable	Reference
Optical photometry	0.3–1 μm	min–years	Extinction/accretion/spots	Δ_m, colour	[3, 31, 32, 41]
Near-IR photometry	~1–5 μm	days–years	Inner dust	ΔF_λ, colour	[11, 32, 39, 50]
Mid/Far-IR	~5–100+ μm	days–years	Cooler dust	IR flux, SED	[32, 39, 43, 50]
UV	~0.1–0.3 μm	min–days	Hot accretion/activity	UV flux	[35, 57]
X-ray	~0.1–10 keV	seconds–years	Magnetic activity	L_X, flare amplitude	[35, 36]
Spectroscopy	wavelength dependent	hours–years	Accretion/outflow/extinction	EW, line profile, RV	[33, 48, 49,]
Polarimetry	optical/NIR	hours–years	Scattering geometry	P, PA	[20, 25, 45, 46]

A useful quantitative example is the Pelican Nebula monitoring study: 90 nights, >250 epochs, and 95 variables, including 67 pre-main-sequence variables; nearly 30% showed strong periodic signatures [44].

4.5. Connecting observations with radiative-transfer models

Observations become physically useful when they can be connected to model parameters. Radiative-transfer calculations can convert a specified stellar luminosity, dust distribution, optical depth, temperature structure, and viewing geometry into predicted SEDs, wavelength-dependent fluxes, polarization, and time-dependent responses [5], [19], [29]. The increasing dimensionality and temporal complexity of radiative-transfer approaches determine their ability to represent realistic circumstellar structures and evolving radiation fields, as summarized in Figure 4 [19], [23], [29].

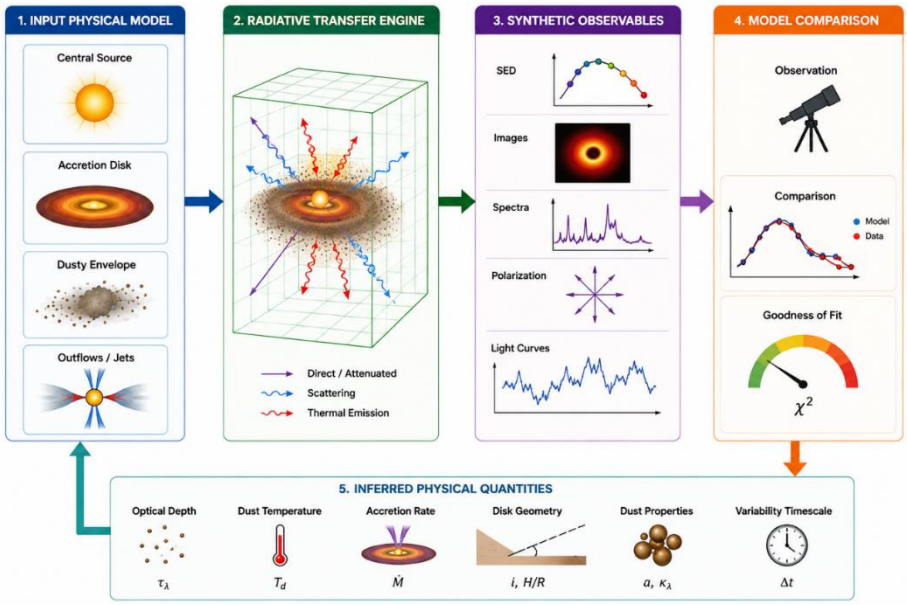

Fig. 4: Hierarchy of Radiative-Transfer Modelling Approaches for Variable Young Stellar Systems, from 1D Radial to Time-Dependent Coupled Models, With Increasing Treatment of Circumstellar Geometry, Scattering, and Temporal Evolution.

The comparison is not simply a forward modelling problem. The observations are used to constrain the model parameters through an inverse process:

Observations → model comparison → physical parameters

For example, optical dimming can constrain extinction, infrared variability can constrain dust temperature and emitting area, polarization can constrain scattering geometry, and emission-line changes can constrain the gas component [56]. Combining these constraints reduces the range of models capable of reproducing the observations [45], [48].

The choice of radiative-transfer method affects the physical information that can be extracted. One-dimensional models provide efficient calculations of radial temperature structures and SEDs but impose strong geometric assumptions [19]. Two-dimensional axisymmetric models provide a better representation of disks but cannot reproduce fully asymmetric structures [19], [29]. Three-dimensional Monte Carlo methods can treat complex geometries and calculate quantities such as images, SEDs, dust temperatures, and polarization [19], [29]. When coupled to atomic-line radiative transfer, these methods can also predict emission-line observables [56]. Time-dependent Monte Carlo approaches extend this framework to variable radiation fields and evolving thermal emission [23].

4.6. Comparative assessment of public radiative-transfer codes

Specific code comparison is more informative than comparing model categories alone. The following assessment separates native capabilities from workflows that require repeated snapshots or external coupling.

Table 4: Comparative assessment of selected public radiative-transfer and thermo-chemical codes relevant to young stellar systems

Code / approach	Geometry & RT	Time-dependent illumination	Dust / sublimation	Gas lines / non-LTE
RADMC-3D [83]	3D Monte Carlo continuum; scattering and ray tracing; gas/molecular line transfer	Primarily snapshot-based; variable illumination can be represented by repeated models, but native coupled thermal time evolution is not its standard workflow	Dust temperature and continuum/scattering; sublimation front must be prescribed or iterated externally	LTE and approximate non-LTE/LVG options; not a thermo-chemical evolution solver
HOCHUNK3D [84]	3D dust RT for YSOs; warps, spirals, clumps,	Can represent source hotspots and changing configurations through	Multiple dust species, stratification prescriptions and puffed-up inner rims;	Primarily continuum/dust

	misaligned disks and hotspots	separate model runs; not a general time-dependent radiation-hydrodynamics solver	sublimation evolution requires external prescription	emission and scattering; not a full thermo-chemical non-LTE disk solver
MCFOST [85, 86]	3D Monte Carlo continuum and line RT; scattered light, thermal emission, polarization and line observables	Standard use is equilibrium/snapshot modelling; temporal variability is generally handled by separate model snapshots rather than a native time-dependent illumination solver	Dust temperature, stochastic heating of small grains, grain populations; moving sublimation fronts require external time sequencing	Atomic/molecular line transfer capabilities; not a coupled thermo-chemical evolution framework
ProDiMo [14, 87]	2D axisymmetric thermo-chemical disk model with continuum RT	Steady or iteratively converged disk states; explicit time-dependent source response is not the primary standard mode	Coupled dust RT, gas heating/cooling and chemistry; dust evolution/sublimation treatment depends on adopted physical prescriptions	Strongest of the four for coupled gas chemistry, thermal balance and non-LTE line modelling
POLARIS time-dependent extension [67]	3D Monte Carlo continuum with scattering and thermal re-emission	Explicitly follows variable illuminating sources and thermal response on finite time steps	Time-dependent dust temperature, scattering and thermal re-emission; suited to variable dusty environments	Primarily continuum/dust; not a complete thermo-chemical gas-dynamics solver

The main radiative-transfer and coupled modelling approaches used to describe circumstellar environments are compared in Table 4, with emphasis on geometry, time dependence, predicted observables, and computational limitations.

The ≤10% benchmark difference is particularly valuable because it gives us a real quantitative statement rather than vague wording about model reliability [19]. Recent time-dependent Monte Carlo work also specifically enables the calculation of evolving thermal re-emission and light-echo behaviour for variable sources [23], [56]. Benchmark comparisons of continuum radiative-transfer codes show generally good agreement in dust-temperature structures, with temperature differences typically below about 10% for the tested configurations, although discrepancies can become larger for SEDs and images in optically thick cases [19].
The theory–observation connection can be represented as:

Variable radiation source → circumstellar response → radiative transfer → observable variability → physical parameter estimation

The reverse process forms the inverse problem. Observed light curves, spectra, infrared emission, and polarization are compared with model predictions to constrain optical depth, dust temperature, disk geometry, accretion activity, and related parameters [19], [29].
The comparison shows that the commonly used public codes do not provide identical forms of time dependence. RADMC-3D, HOCHUNK3D and MCFOST are powerful three-dimensional dust-radiative-transfer tools, but a variable source is normally represented by a sequence of model states unless an external time-stepping framework is supplied. HOCHUNK3D is particularly useful for complex YSO geometries and accretion hotspots, while MCFOST provides continuum, polarization and line-transfer capabilities. RADMC-3D is flexible for continuum and molecular-line post-processing on arbitrary three-dimensional density structures [83–86].
ProDiMo occupies a different part of the modelling space. It couples two-dimensional dust radiative transfer with gas heating and cooling, chemistry, hydrostatic structure and non-LTE molecular/atomic line calculations. Its strength is the coupled gas–dust thermochemical problem rather than explicit light-travel-time evolution of a variable source [87]. For an intrinsically time-dependent illumination problem, a practical workflow is therefore to combine a time-dependent continuum solver such as the POLARIS implementation with a thermo-chemical model or to generate a sequence of physical states and pass them through a line-transfer calculation [67].
Dust sublimation fronts are not automatically equivalent to time-dependent radiative transfer. A code may calculate the instantaneous dust temperature while leaving the grain removal, re-condensation and redistribution prescription external to the radiative-transfer calculation. This distinction is important when interpreting near-infrared lags or changes in the inner-rim radius. The appropriate benchmark should consequently compare not only SED agreement but also temperature response, optical-depth evolution, polarization, and the temporal response function under the same variable illumination history.

4.6. Critical synthesis

The diagnostics discussed above constrain different parts of the same physical system. Photometry gives the temporal and amplitude information, spectroscopy adds information about gas emission and velocity structure, infrared observations trace dust temperature and geometry, and polarimetry constrains scattering geometry [45], [48], [57]. Their diagnostic power increases when the measurements are simultaneous or obtained with sufficiently matched temporal sampling.
A practical interpretation can be framed through four quantities: [60]

$$\{\Delta m\ \Delta F_{\lambda} EW\ P\} \tag{10}$$

together with the characteristic timescale Δt. A change in Δm alone has several possible explanations. Adding colour constrains the wavelength dependence, EW tests the gas response, infrared flux tests the dust response, and P provides geometric information. The combination narrows the set of physically consistent interpretations [60].
This also exposes an important limitation in current observational studies. Different datasets often have different cadence, wavelength coverage, and temporal baselines. A high-cadence optical light curve may not have simultaneous infrared or spectroscopic coverage. The physical connection between observed bands can then remain uncertain even when the individual datasets are of high quality [28], [32], [43].
Radiative-transfer modelling can bridge this gap by predicting several observables from the same physical configuration. A model that reproduces only the optical light curve does not provide a strong physical constraint if several combinations of luminosity, extinction, and geometry can produce the same result. A stronger test requires simultaneous agreement with multiple observables, such as optical amplitude, infrared response, emission-line behaviour, and polarization [19], [29].
The main research need is therefore not simply a larger number of observations or more complex models. It is the development of coordinated time-domain datasets and models that treat radiation, dust, gas, and geometry as coupled components. This approach can move the interpretation from identifying variability patterns towards estimating the physical parameters responsible for those patterns [29, 32,43]. This provides the basis for the next section, where radiative-transfer and coupled modelling approaches are compared in greater detail with emphasis on geometry, temporal evolution, predictive capability, and remaining limitations.

5. Challenges and Future Perspectives

The interpretation of variability in young stellar systems involves several physical processes operating at the same time. Stellar activity, accretion, dust extinction, scattering, dust evolution, and disk dynamics can produce similar changes in brightness and colour. A decrease in observed optical flux, for example, may result from a lower intrinsic luminosity, reduced accretion emission, increased optical depth, or a change in the scattering geometry. Photometry alone cannot separate these possibilities.

5.1. Three-dimensional circumstellar structure

Many radiative-transfer calculations use simplified geometries to control computational cost. These approximations are useful when the main objective is to examine radial temperature distributions or broad spectral-energy-distribution behaviour. Real circumstellar disks can contain warps, clumps, gaps, spiral structures, asymmetric illumination, and spatially varying dust populations. These structures modify the path length, optical depth, scattering probability, and emitting area seen by the observer [30], [63]. The limitation can be expressed through measurable geometric quantities such as disk aspect ratio H/R, inclination i, clump size R_{cl} ,and radial location R_{cl} / R_{in} . A useful modelling target is therefore not simply a more complex geometry, but a geometry whose parameters can be constrained by observations.
Three-dimensional radiative-transfer calculations provide a route for this problem. They can test whether changes in brightness, colour, infrared flux, or polarization can be reproduced by a particular non-axisymmetric structure. Models incorporating inner-disk warps, hotspots, and clumpy density structures have demonstrated that changes in three-dimensional geometry can produce distinct optical and infrared variability signatures [61]. Recent radiative-transfer studies further show that non-axisymmetric structures can generate observable shadows and spatially varying scattered-light signatures, providing a direct link between disk geometry and measurable observables [62]. The main restriction is computational demand, especially when the geometry must evolve with time

5.2. Dust evolution and variable opacity

Dust is often represented using fixed grain properties, while the radiation field itself can vary on timescales much shorter than the evolution of the dust population. This assumption can become restrictive when heating approaches the sublimation regime or when dust is redistributed through the disk [64]. The relevant parameters include grain radius α_{grain}, sublimation temperature T_{sub} ,dust mass M_{dust} ,opacity $k\lambda$, and the spatial dust density $\rho_{dust}(r, t)$. Changes in these quantities modify both absorption and thermal emission. A time-dependent treatment should therefore allow quantities such as [65]

$$k_{\lambda} = k_{\lambda}\ (\alpha_{grain}\ t) \tag{11}$$

And

$$\rho_{dust} = \rho_{dust}(r, \theta, \phi, t) \tag{12}$$

to evolve when the physical conditions require it. This is particularly relevant to variable inner disks. A change in luminosity can alter dust temperature, which can modify the sublimation boundary, which then changes the amount of dust available to intercept radiation [22]. The radiation field and dust distribution are therefore coupled variables rather than independent inputs [64].

5.3. Temporal response and non-steady behaviour

Steady-state radiative-transfer models provide a useful solution for a fixed radiation field and fixed circumstellar structure. They do not directly describe the response following a rapid change in luminosity or accretion rate. For a variable source, the observationally relevant quantities include the time delay [23]

$$\Delta t = t_{response} - t_{source,} \tag{13}$$

the response amplitude

$$A_{re} = \frac{\Delta F_{resp}}{F_{baseline}}, \tag{14}$$

and the temporal response function R(t).These quantities allow the model to be compared directly with time-domain observations [23]. An optical event followed by infrared emission, for example, can be represented as a convolution between the source variability and the response of the circumstellar dust: [66]

$$F_{IR} = \int R(\tau)\, F_{source}(t-\tau)\, d\tau \tag{15}$$

The shape of R(t) contains information about the spatial extent and thermal response of the emitting material. A narrow response indicates a relatively compact or sharply defined emitting region, while a broad response can arise from an extended dust distribution or a range of light-travel and thermal timescales [52, 66]. Time-dependent Monte Carlo radiative-transfer methods are particularly relevant here because they can follow evolving radiation fields and thermal re-emission rather than calculating only a static equilibrium configuration [67].

5.4. Intrinsic variability versus variable extinction

One of the hardest observational problems is separating changes in the central radiation source from changes in circumstellar extinction. The same decrease in optical flux can be produced by different physical mechanisms.
A useful diagnostic set is [13]

$$\{\Delta m, \Delta(B-V)\ P, EW, \Delta F_{IR}\} \tag{16}$$

Here, Δm measures brightness variation, colour change provides information on wavelength-dependent extinction, P constrains scattering, EW traces the gas component, and infrared variation probes the dust response [13].
The interpretation becomes stronger when these observables are obtained simultaneously. A dimming event accompanied by reddening and enhanced linear polarization is generally consistent with increased circumstellar obscuration and scattering, although polarization alone is not uniquely diagnostic because changes in the disc or wind geometry can also modify the polarized flux [6], [11], [13]. A brightness increase accompanied by enhanced accretion-sensitive emission lines and ultraviolet excess is more consistent with increased accretion activity [13]. Recent multi-epoch VVV observations further demonstrate that high-amplitude YSO variability can include both episodic accretion events and long-duration extinction events, while near-infrared spectroscopy can distinguish eruptive, accretion-dominated and outflow-dominated states [11], [68].
The same photometric amplitude can therefore correspond to different physical processes, motivating simultaneous multiwavelength photometry, polarimetry and spectroscopy as a mechanism-discrimination strategy rather than relying on variability detection alone [13]. This is why the future observational target should be mechanism discrimination rather than variability detection alone.

5.5. Accretion variability and indirect mass-accretion estimates

Mass-accretion rate is often inferred indirectly from continuum excess or emission-line properties. The uncertainty arises because line emission depends on temperature, density, geometry, ionization, and velocity structure in addition to the accretion rate [71]. A more rigorous time-domain analysis should therefore compare $\Delta\dot{M}, \Delta W, \Delta F_{cont}$ within the same temporal sequence. Time-resolved spectroscopy can test whether changes in line strength follow changes in the continuum and whether the line profile changes at the same time. This distinction is important because continuum variations do not necessarily correspond to equivalent changes in the inferred accretion rate: long-term monitoring of TW Hya, for example, found good correlations between accretion luminosity and He-line luminosity but poor correlations with Hα and Hβ luminosities [70]. Recent simultaneous photometric and spectroscopic monitoring of DR Tau further demonstrates that observed variability can arise from a combination of accretion, winds, stellar activity, and circumstellar obscuration [69]. The research target is therefore a physically constrained estimate of $\dot{M}(t)$, rather than simply assigning an accretion origin to every optical brightening event.

5.6. Model–data mismatch and parameter degeneracy

A model can reproduce an observed light curve using more than one combination of physical parameters. For example, similar optical dimming can be produced by increasing dust optical depth or decreasing intrinsic luminosity. This creates a parameter-degeneracy problem. Such degeneracies are well documented in astrophysical SED and radiative-transfer modelling, and additional wavelength coverage can help distinguish between competing physical interpretations [72], [73]. Model comparison should therefore use several observables simultaneously. Quantitative evaluation can be based on residuals,

$$r_i = \left(\frac{O_i - M_i}{\sigma_i}\right) \tag{17}$$

And a goodness-of-fit statistic,

$$\chi^2 = \sum_i \left(\frac{O_i - M_i}{\sigma_i}\right)^2 \quad (18)$$

Where O_i represents the observation, M_i the model prediction, and Σ_i the observational uncertainty.
Bayesian inference can extend this approach by producing posterior distributions for parameters such as optical depth, disk inclination, dust temperature, inner-rim radius, and accretion rate [74], [75]. This is preferable to reporting a single best-fit model when several parameter combinations remain allowed by the data. This allows parameter correlations and remaining degeneracies to be quantified rather than concealed by a single best-fit solution [72].

5.7. Multiwavelength and coordinated time-domain observations

The lack of simultaneous observations remains a practical limitation. Optical observations trace direct and scattered radiation, infrared observations probe emission from heated circumstellar dust, while ultraviolet and X-ray observations provide complementary constraints on energetic accretion and stellar activity. Coordinated multiwavelength monitoring is therefore important for distinguishing changes in the central source from the subsequent response of the circumstellar environment. Recent observations of eruptive young stellar objects demonstrate the value of combining optical and infrared time series: a measured delay between optical and infrared variability can provide constraints on the location and propagation of an accretion instability [76], [78].
A coordinated campaign should aim to measure:

- optical brightness and colour,
- near- and mid-infrared flux,
- UV and X-ray variability where available,
- emission-line strength and profile,
- polarization degree and position angle,
- optical–IR and high-energy time delays.

The important quantity is not simply the number of observations but the degree of temporal overlap between the datasets. Simultaneous or closely sampled measurements make it possible to test whether variability in different bands is correlated or delayed, thereby distinguishing direct changes in the central source from reprocessing or structural responses in the circumstellar material [39].In particular, measured infrared–optical lags can constrain the radial location at which an instability originates, while long-term infrared monitoring can reveal otherwise missed episodes of protostellar variability [39], [76].

5.8. Machine-learning-assisted time-domain analysis

Large time-domain surveys provide rapidly growing numbers of light curves that cannot be analysed efficiently using manual classification alone. Machine-learning methods can automate the identification of variability patterns, classify light-curve morphologies, and separate populations with different variability behaviour. This approach has already been demonstrated for young stellar objects using TESS light curves and for large-scale time-domain surveys such as ZTF [80], [81]. Recent work further shows that combining infrared photometry with time-domain light-curve information can improve the discrimination of YSOs from astrophysical contaminants [79].
The physical interpretation should, however, remain connected to radiative-transfer models. A machine-learning classifier can identify a light-curve morphology or assign an object to a variability class, but the classification itself does not uniquely determine physical quantities such as dust optical depth, inner-rim radius, or accretion rate. These quantities require a physical forward model and appropriate observational constraints. This distinction is important because similar light-curve morphologies can arise from different physical mechanisms, including changes in accretion, extinction, and stellar surface activity [40].
A useful future workflow is therefore:

Time-domain observations → variability classification → radiative-transfer model library → parameter inference → observational validation

Such a framework is consistent with the broader development of simulation-based inference, in which machine-learning emulators are trained on large libraries of high-fidelity radiative-transfer calculations and subsequently used to accelerate parameter inference. Recent work demonstrates that this approach can generate large numbers of model light curves efficiently while also highlighting the need to test the reliability of the emulator outside its training domain [82]. The major challenges identified in current time-dependent circumstellar studies, together with measurable targets and possible approaches for addressing them, are summarized in Table 5.

Table 5: Current Challenges, Measurable Targets and Future Approaches for Time-Dependent Studies of Young Stellar Systems

Research gap	Present limitation	Quantitative target / measurable quantity	Future approach
3D disk structure	Simplified geometry	Spatial scale in AU / inclination H/R	3D radiative transfer
Dust evolution	Fixed grain properties	α_{grain}, T_{sub}, dust mass	Coupled dust evolution
Temporal response	Steady-state assumptions	Δt, lag, response function	Time-dependent modelling
Intrinsic vs extinction variability	Degenerate light curves	Δm, colour slope, P	Simultaneous photometry + polarimetry
Accretion variability	Indirect $\dot{M}$ estimates	$\Delta\dot{M}$, line EW, continuum excess	Time-resolved spectroscopy
Model–data mismatch	Parameter degeneracy	χ^2, residuals, posterior distributions	Bayesian inference
Multiwavelength coupling	Sparse simultaneous datasets	Optical–IR/X-ray lag	Coordinated campaigns
Model validation	Code/model dependence	Flux/temperature residual (%)	Benchmark datasets

5.9. Future research framework

A useful research framework combines three components: coordinated multiwavelength observations, time-dependent radiative-transfer calculations, and physical parameter inference.

Observations → Time-dependent RT → parameter inference → Prediction → observational test

The framework changes the role of modelling from post-processing observations to testing physical explanations. A model should predict measurable quantities such as optical amplitude, infrared lag, spectral-line response, polarization, or SED evolution. These predictions can then be compared with new observations. Machine-learning methods may also assist the analysis of large time-domain datasets by identifying variability patterns and comparing observations with libraries of physical models. Their application should remain connected to physically interpretable radiative-transfer calculations so that identified patterns can be related to measurable properties of the star–disk system. A future framework that combines multiwavelength time-domain observations, time-dependent radiative-transfer modelling, and physical parameter inference can provide a direct connection between variable radiation and the evolving circumstellar environment, as illustrated in Figure 5.

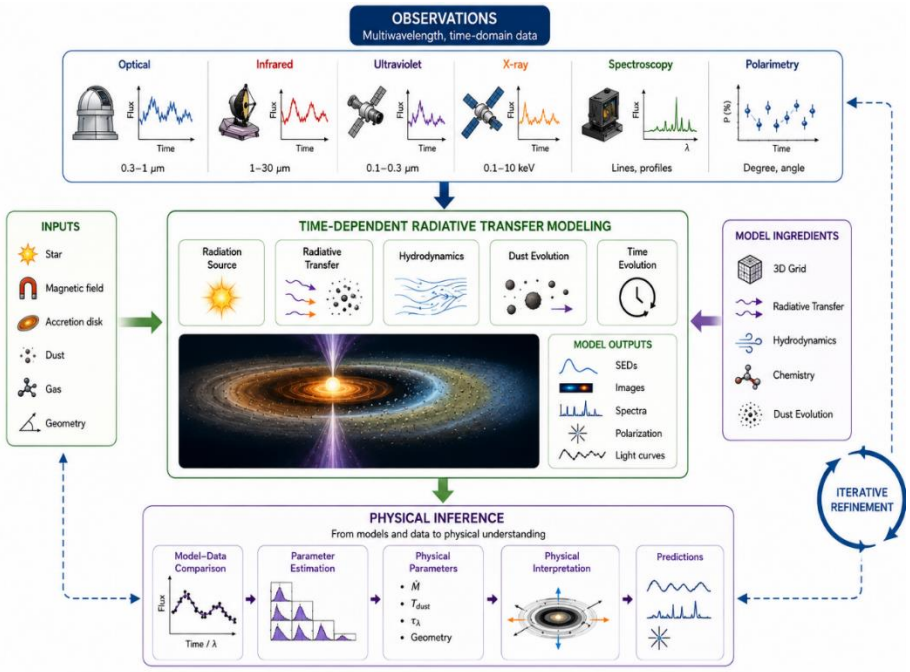

Fig. 5: Future Research Framework Integrating Multiwavelength Time-Domain Observations, Time-Dependent Radiative-Transfer Modelling, and Physical Inference for Evolving Circumstellar Environments.

The main modelling priorities are three-dimensional radiation–matter coupling, evolving dust properties, multiwavelength emission, and predictions that can be tested observationally.

5.10. Critical synthesis

The main limitation in the present field is not the absence of individual observational or modelling techniques. The problem is the incomplete connection between them. Photometry can identify variability, spectroscopy can identify changes in gas emission, infrared observations can trace dust response, and polarimetry can constrain geometry. Yet these datasets are often obtained with different temporal coverage and are interpreted using models with different assumptions. The next stage of work should treat radiation, dust, gas, and disk structure as coupled components. The measurable targets are already identifiable: H/R, i, T_{sub}, M_{dust}, $k\lambda$, Δt, P, EW, $\dot{M}$, residuals, and posterior parameter distributions.

Future models should not only reproduce an observed light curve; they should reproduce several observables from the same physical configuration and make predictions that can be tested with coordinated observations. The resulting framework connects variable radiation at the central source with the evolving circumstellar environment and, finally, with the signals measured by an observer. This approach can move the field from phenomenological classification of variability towards quantitative inference of the physical conditions governing young stellar systems.

6. Conclusion

Young stellar systems provide a useful environment for studying time-dependent radiation–matter interactions because stellar radiation, accretion, circumstellar gas, dust, and disk structures evolve over different spatial and temporal scales. The observed variability is not controlled by the central source alone. Absorption, scattering, thermal re-emission, dust sublimation, optical-depth variation, and structural changes within the circumstellar environment can alter the radiation before it reaches the observer. A physical interpretation of variability must consequently consider the source and its surrounding material as a coupled system.

This review examined the physical basis of radiative transfer, the mechanisms responsible for variability, the observational signatures associated with these mechanisms, and the modelling approaches used to describe evolving young stellar systems. Accretion variability, stellar activity, variable extinction, scattering, dust evolution, and disk-structure changes can produce similar photometric behaviour. Photometric amplitude alone is not sufficient to distinguish these processes. Colour variation, emission-line strength and profile, infrared emission, polarization, and temporal delays provide additional constraints on the origin of the observed variability. The temporal response of circumstellar material is a key component of this interpretation. A change in the radiation field can produce delayed emission through light-travel effects, dust heating and cooling, sublimation, condensation, and changes in optical depth. The delay between variations observed at different wavelengths can provide information about the location and physical response of the emitting material. Time-dependent

radiative-transfer calculations are suited to this problem because they can follow changes in the radiation field and the subsequent response of the circumstellar environment.

A central outcome of this review is the source–response–observable framework, which connects variable radiation from the central source with radiation–matter interaction, circumstellar response, multiwavelength observables, and physical parameter inference. Within this framework, photometric amplitude, colour variation, emission-line equivalent width, polarization, infrared flux variation, and temporal lag can be related to optical depth, dust temperature, disk geometry, inner-rim location, and accretion activity. This approach provides a physical basis for moving from the identification of variability towards quantitative interpretation of the processes responsible for it.

The comparison of radiative-transfer approaches shows that model complexity should be selected according to the physical problem being investigated. One-dimensional and axisymmetric models remain useful for controlled studies of temperature structure and spectral-energy distributions. Three-dimensional models become necessary when asymmetric structures, non-uniform illumination, complex scattering, or spatially varying dust distributions influence the observable radiation. Time-dependent calculations are required when the source variability and circumstellar response occur on comparable timescales. The main sources of uncertainty include simplified geometries, fixed dust properties, steady-state assumptions, parameter degeneracy, and incomplete multiwavelength coverage.

Future studies can address these limitations through coordinated time-domain observations combined with time-dependent radiative-transfer modelling. Optical and ultraviolet observations can trace changes in the stellar and accretion components, spectroscopy can probe circumstellar gas, infrared observations can follow dust heating, and polarimetry can constrain scattering geometry. Simultaneous measurements across these wavelength regimes can provide a stronger physical constraint than independent analysis of individual datasets.

A useful modelling strategy is to require a single physical configuration to reproduce several observables at the same time. Photometric amplitude, colour, emission-line behaviour, infrared response, polarization, and temporal lag can then be evaluated together rather than fitted independently. Bayesian parameter inference and quantitative residual analysis can further identify which combinations of dust properties, geometry, optical depth, and accretion parameters remain consistent with the observations.

Time-dependent radiation–matter interaction offers a physical route for interpreting variability as a diagnostic of evolving star–disk environments. The combination of multiwavelength observations, time-dependent radiative-transfer calculations, and quantitative parameter inference can provide constraints on the structure and evolution of circumstellar material that cannot be obtained from single-band variability alone. This integrated approach can support future studies aimed at resolving the connection between variable stellar radiation, circumstellar dust and gas, and the observable evolution of young stellar systems.

Acknowledgement

The author gratefully acknowledges the use of open-access scientific literature, publicly available research articles, and standard scientific resources that contributed to the development of the theoretical framework presented in this study. The authors also appreciate the efforts of the scientific community in making space physics and astrophysical research widely accessible.

References

[1] Waters, L. B. F. M., & Waelkens, C. (1998). Herbig Ae/Be stars. Annual Review of Astronomy and Astrophysics, 36, 233–266. https://doi.org/10.1146/annurev.astro.36.1.233.

[2] Brittain, S. D., Kamp, I., Meeus, G., et al. (2023). Herbig Stars: A Quarter Century of Progress. Space Science Reviews, 219(1), 7. https://doi.org/10.1007/s11214-023-00949-z.

[3] Cody, A. M., Hillenbrand, L. A., Chandragiri, S., & Morgan, M. (2025). The Optical Photometric Variability of Herbig Ae/Be Stars from TESS. The Astrophysical Journal, 994, 253. https://doi.org/10.3847/1538-4357/ae119a.

[4] Wichittanakom, C., Oudmaijer, R. D., Fairlamb, J. R., Mendigutía, I., Vioque, M., & Ababakr, K. M. (2020). The accretion rates and mechanisms of Herbig Ae/Be stars. Monthly Notices of the Royal Astronomical Society, 493(1), 234–249. https://doi.org/10.1093/mnras/staa169.

[5] Pezzuto, S., Strafella, F., & Lorenzetti, D. (1997). On the circumstellar matter distribution around Herbig Ae/Be Stars. The Astrophysical Journal, 485(1), 290–307. https://doi.org/10.1086/304398.

[6] Ribas, Á., Vioque, M., Zagaria, F., et al. (2025). A young gas giant and hidden substructures in a protoplanetary disk. Nature Astronomy, 9, 1176–1183. https://doi.org/10.1038/s41550-025-02576-w.

[7] Kowalski, A. F. (2024). Stellar flares. Living Reviews in Solar Physics, 21, 1. https://doi.org/10.1007/s41116-024-00039-4.

[8] Vink, J. S., Drew, J. E., Harries, T. J., & Oudmaijer, R. D. (2002). Probing the circumstellar structure of Herbig Ae/Be stars. Monthly Notices of the Royal Astronomical Society, 337, 356–368. https://doi.org/10.1046/j.1365-8711.2002.05920.x.

[9] Mendigutía, I., Eiroa, C., Montesinos, B., et al. (2011). Optical spectroscopic variability of Herbig Ae/Be stars. Astronomy & Astrophysics, 529, A34. https://doi.org/10.1051/0004-6361/201015821.

[10] Ababakr, K. M., Oudmaijer, R. D., & Vink, J. S. (2016). Linear spectropolarimetry across the optical spectrum of Herbig Ae/Be stars. Monthly Notices of the Royal Astronomical Society, 461(3), 3089–3110. https://doi.org/10.1093/mnras/stw1534.

[11] Guo, Z., Lucas, P. W., Contreras Peña, C., et al. (2021). Analysis of physical processes in eruptive YSOs with near-infrared spectra and multiwavelength light curves. Monthly Notices of the Royal Astronomical Society, 504, 830–856. https://doi.org/10.1093/mnras/stab882.

[12] Wang, X.-L., Fang, M., Herczeg, G. J., et al. (2023). Variability of Young Stellar Objects in the Perseus Molecular Cloud. Research in Astronomy and Astrophysics, 23(7), 075015. https://doi.org/10.1088/1674-4527/acd58b.

[13] Fischer, W. J., Hillenbrand, L. A., Herczeg, G. J., Johnstone, D., Kóspál, Á., & Dunham, M. M. (2022). Accretion Variability as a Guide to Stellar Mass Assembly. 9, 355. https://doi.org/10.26624/EXEY2927.

[14] Öberg, K. I., Facchini, S., & Anderson, D. E. (2023). Protoplanetary Disk Chemistry. Annual Review of Astronomy and Astrophysics, 61, 287–328. https://doi.org/10.1146/annurev-astro-022823-040820.

[15] Natta, A., Prusti, T., Neri, R., Wooden, D., Grinin, V. P., & Mannings, V. (2001). A reconsideration of disk properties in Herbig Ae stars. Astronomy & Astrophysics, 371, 186–197. https://doi.org/10.1051/0004-6361:20010334.

[16] Draine, B. T. (2003). Interstellar Dust Grains. Annual Review of Astronomy and Astrophysics, 41, 241–289. https://doi.org/10.1146/annurev.astro.41.011802.094840.

[17] Andrews, S. M. (2020). Observations of Protoplanetary Disk Structures. Annual Review of Astronomy and Astrophysics, 58, 483–528. https://doi.org/10.1146/annurev-astro-031220-010302.

[18] Dullemond, C. P., & Monnier, J. D. (2010). The Inner Regions of Protoplanetary Disks. Annual Review of Astronomy and Astrophysics, 48, 205–239. https://doi.org/10.1146/annurev-astro-081309-130932.

[19] Pinte, C., Ménard, F., Duchêne, G., & Bastien, P. (2006). Monte Carlo radiative transfer in protoplanetary disks. Astronomy & Astrophysics, 459, 797–804. https://doi.org/10.1051/0004-6361:20053275.

[20] Grinin, V. P., & Tambovtseva, L. V. (2022). Scattered Radiation of Protoplanetary Disks. Universe, 8, 224. https://doi.org/10.3390/universe8040224.

[21] Kama, M., Min, M., & Dominik, C. (2009). The inner rim structures of protoplanetary discs. Astronomy & Astrophysics, 506, 1199–1213. https://doi.org/10.1051/0004-6361/200912068.

[22] Xu, S., Wang, L., Ho, L. C., Cen, R., & Xu, S. (2026). Consistent Modeling of Nonequilibrium Dust Sublimation and the Interactions with Dust Evolution in the Inner Regions of Protoplanetary Disks. The Astrophysical Journal, 997, 14. https://doi.org/10.3847/1538-4357/ae2683.

[23] D T, Ayswarya Lakshmi, and Ranjith R. 2026. "A Unified Analytical Framework for Nonlinear Plasma Instabilities and Magnetic Reconnection During Geomagnetic Substorm Evolution". *International Journal of Advanced Astronomy* 14 (1): 16-29. https://doi.org/10.14419/qppe5m63.

[24] Brunngräber, R., & Wolf, S. (2020). Self-scattering in protoplanetary disks with dust settling. Astronomy & Astrophysics, 640, A122. https://doi.org/10.1051/0004-6361/202037981.

[25] Min, M., Canovas, H., Mulders, G. D., & Keller, C. U. (2012). The effects of disk and dust structure on observed polarimetric images of protoplanetary disks. Astronomy & Astrophysics, 537, A75. https://doi.org/10.1051/0004-6361/201117333.

[26] Brunngräber, R., & Wolf, S. (2019). Polarization reversal of scattered thermal dust emission in protoplanetary disks at submillimetre wavelengths. Astronomy & Astrophysics, 627, L10. https://doi.org/10.1051/0004-6361/201935169.

[27] Tazaki, R., Tanaka, H., Kataoka, A., Okuzumi, S., & Muto, T. (2019). Unveiling Dust Aggregate Structure in Protoplanetary Disks by Millimeter-wave Scattering Polarization. The Astrophysical Journal, 885, 52. https://doi.org/10.3847/1538-4357/ab45f0.

[28] Vinković, D. (2014). Constraints on the height of the inner disk rim in pre-main-sequence stars. Astronomy & Astrophysics, 566, A117. https://doi.org/10.1051/0004-6361/201322008.

[29] Villenave, M., Rosotti, G. P., Lambrechts, M., Ziampras, A., Pinte, C., Ménard, F., Stapelfeldt, K. R., Duchêne, G., Baylock, E., & Doi, K. (2025). Turbulence in protoplanetary disks: A systematic analysis of dust settling in 33 disks. Astronomy & Astrophysics, 697, A64. https://doi.org/10.1051/0004-6361/202553822.

[30] Whitney, B. A., Robitaille, T. P., Bjorkman, J. E., Dong, R., Wolff, M. J., Wood, K., & Honor, J. (2013). Three-Dimensional Radiation Transfer in Young Stellar Objects. The Astrophysical Journal Supplement Series, 207, 30. https://doi.org/10.1088/0067-0049/207/2/30.

[31] Lakeland, B. S., & Naylor, T. (2022). Towards an understanding of YSO variability: a multiwavelength analysis of bursting, dipping, and symmetrically varying light curves of disc-bearing YSOs. Monthly Notices of the Royal Astronomical Society, 514(2), 2736–2755. https://doi.org/10.1093/mnras/stac1477.

[32] Lee, S., Lee, J.-E., Contreras Peña, C., Johnstone, D., Herczeg, G., & Lee, S. (2024). Mid-infrared Variability of Young Stellar Objects on Timescales of Days to Years. The Astrophysical Journal, 962(1), 38. https://doi.org/10.3847/1538-4357/ad14f8.

[33] Contreras Peña, C., Herczeg, G. J., Ashraf, M., Jose, J., Lee, H.-G., Johnstone, D., Lee, J.-E., Zhou, X.-Y., Liu, H., & Yoon, S.-Y. (2023). Photometric and spectroscopic monitoring of YSOs in nearby star-forming regions – I. Eruptive YSOs. Monthly Notices of the Royal Astronomical Society, 521(4), 5669–5685. https://doi.org/10.1093/mnras/stad820.

[34] Contreras Peña, C., Lucas, P. W., Guo, Z., Smith, L., (2024). On the incidence of episodic accretion in Class I YSOs from VVV. Monthly Notices of the Royal Astronomical Society, 528(2), 1823–1840. https://doi.org/10.1093/mnras/stad3780.

[35] Feinstein, A. D., Seligman, D. Z., France, K., Gagné, J., & Kowalski, A. (2024). Evolution of Flare Activity in GKM Stars Younger Than 300 Myr over Five Years of TESS Observations. The Astronomical Journal, 168(2), 60. https://doi.org/10.3847/1538-3881/ad4edf.

[36] Seli, B., Vida, K., Oláh, K., Görgei, A., Soós, Sz., Pál, A., Kriskovics, L., & Kővári, Zs. (2025). Stellar flare morphology with TESS across the main sequence. Astronomy & Astrophysics, 694, A161. https://doi.org/10.1051/0004-6361/202452489.

[37] Shulman, S. G., & Grinin, V. P. (2022). UX Ori stars eclipses by large-scale disc perturbations. Monthly Notices of the Royal Astronomical Society, 512(2), 3098–3112. https://doi.org/10.1093/mnras/stac667.

[38] Fukuhara, Y., & Okuzumi, S. (2024). A self-consistent model for dust settling and the vertical shear instability in protoplanetary disks. Publications of the Astronomical Society of Japan, 76(4), 708–719. https://doi.org/10.1093/pasj/psae042.

[39] Morris, C., Guo, Z., Lucas, P. W., Miller, N., Contreras Peña, C., & Kuhn, M. A. (2025). Eruptive YSOs in Cygnus-X: a mid-infrared variability study with NEOWISE and spicy. Monthly Notices of the Royal Astronomical Society, 537(3), 2763–2781. https://doi.org/10.1093/mnras/staf079.

[40] Ryan, B. W., Stokes-Geddes, H., & Froebrich, D. (2025). A survey for variable young stars with small telescopes – X. Comparing stochastic YSO light curves. Monthly Notices of the Royal Astronomical Society, 543(2), 1133–1145. https://doi.org/10.1093/mnras/staf1495.

[41] Borissova, J., Kurtev, R., Escobar, J., Alonso-García, J., Medina, N., Osses, J., Guo, Z., et al. (2025). Young Stellar Objects in the Carina nebula: Near-Infrared variability and spectroscopy. The Astronomical Journal, 170(3), 135. https://doi.org/10.3847/1538-3881/adeb7d.

[42] Birnstiel, T. (2024). Dust Growth and Evolution in Protoplanetary Disks. Annual Review of Astronomy and Astrophysics, 62, 157–202. https://doi.org/10.1146/annurev-astro-071221-052705.

[43] Kulkarni, C. S., Behling, T., Banks, E. E., Jones, J., Robbins, T., Burns-Watson, N., Megeath, S. T., et al. (2026). 27 yr of Spaceborne IR Astronomy: An ISO, Spitzer, WISE, and NEOWISE Survey for Large-amplitude Variability in Young Stellar Objects. The Astrophysical Journal, 1000(2), 188. https://doi.org/10.3847/1538-4357/ae3156.

[44] Bhardwaj, A., Panwar, N., Herczeg, G. J., Chen, W. P., & Singh, H. P. (2019). Variability of young stellar objects in the star-forming region Pelican Nebula. Astronomy & Astrophysics, 627, A135. https://doi.org/10.1051/0004-6361/201935418.

[45] Ren, B. B., Benisty, M., Ginski, C., Tazaki, R., Wallack, N. L., Milli, J., Garufi, A., Bae, J., Facchini, S., Ménard, F., Pinilla, P., Swastik, C., Teague, R., & Wahhaj, Z. (2023). Protoplanetary disks in Ks band total intensity and polarized light. Astronomy & Astrophysics, 680, A114. https://doi.org/10.1051/0004-6361/202347353.

[46] Ma, J., Schmid, H. M., & Stolker, T. (2024). Color measurements of the polarized light scattered by dust in protoplanetary disks. Astronomy & Astrophysics, 683, A18. https://doi.org/10.1051/0004-6361/202347782.

[47] Harrison, R. E., Lin, Z.-Y. D., Looney, L. W., Li, Z.-Y., Yang, H., Stephens, I. W., & Fernández-López, M. (2024). Protoplanetary Disk Polarization at Multiple Wavelengths: Are Dust Populations Diverse? The Astrophysical Journal, 967(1), 40. https://doi.org/10.3847/1538-4357/ad39ec.

[48] Shridharan, B., Manoj, P., Pathak, V. C., Caratti o Garatti, A., Banerjee, B., Henning, Th., Kamp, I., et al. (2026). Improving accretion diagnostics for young stellar objects with mid-infrared hydrogen lines from JWST/MIRI. Astronomy & Astrophysics, 708, A22. https://doi.org/10.1051/0004-6361/202556384.

[49] Rogers, C., Brandl, B., & de Marchi, G. (2025). Kinematic evidence of magnetospheric accretion for Herbig Ae stars with JWST NIRSpec. Astronomy & Astrophysics, 698, A226. https://doi.org/10.1051/0004-6361/202453356.

[50] Sharma, N., & Sharma, S. (2025). Illuminating Youth: Decades of Mid-infrared Variability and Color Evolution of Young Stellar Objects. The Astrophysical Journal Supplement Series, 278(1), 10. https://doi.org/10.3847/1538-4365/adc397.

[51] Varga, J., Gabányi, K. É., Ábrahám, P., Chen, L., Kóspál, Á., Menu, J., Ratzka, Th., et al. (2017). Mid-infrared interferometric variability of DG Tauri: Implications for the inner-disk structure. Astronomy & Astrophysics, 604, A84. https://doi.org/10.1051/0004-6361/201630287.

[52] Guise, E., Hönig, S. F., Gorjian, V., Barth, A. J., Almeyda, T., Pei, L., Cenko, S. B., Edelson, R., Filippenko, A. V., Joner, C. D., Laney, C. D., Li, W., Malkan, M. L., Nguyen, M. L., & Zheng, W. (2022). Dust reverberation mapping and light-curve modelling of Zw229-015. Monthly Notices of the Royal Astronomical Society, 516(4), 4898–4915. https://doi.org/10.1093/mnras/stac2529.

[53] Nixon, M. C., & Madhusudhan, N. (2022). Aura-3D: A three-dimensional atmospheric retrieval framework for exoplanet transmission spectra. The Astrophysical Journal, 935(2), 73. https://doi.org/10.3847/1538-4357/ac7c09.

[54] Barbosa Martins, V., Mitjans, N. J., Garrappa, S., Franckowiak, A., Ofek, E. O., Ben-Ami, S., Borowska-Naguszewska, J., et al. (2026). Science with a large field-of-view polarization survey: The Large Array Survey Telescope Polarization Node (LAST-P). Publications of the Astronomical Society of the Pacific, 138(1), 015002. https://doi.org/10.1088/1538-3873/ae33f3.

[55] Roumesy, M., Ménard, F., Duchêne, G., Tazaki, R., & Ginski, C. (2026). Probing dust properties through polarized scattered-light images of a sample of ring-shaped protoplanetary disks. Astronomy & Astrophysics, 710, A75. https://doi.org/10.1051/0004-6361/202659540.

[56] Tessore, B., Pinte, C., Bouvier, J., & Ménard, F. (2021). Atomic line radiative transfer with MCFOST: I. Code description and benchmarking. Astronomy & Astrophysics, 647, A27. https://doi.org/10.1051/0004-6361/202039697.

[57] Wendeborn, J., Espaillat, C. C., Lopez, S., Thanathibodee, T., Robinson, C. E., et al. (2024). A Multiwavelength, Multiepoch Monitoring Campaign of Accretion Variability in T Tauri Stars from the ODYSSEUS Survey. I. HST Far-UV and Near-UV Spectra. The Astrophysical Journal, 970(2), 118. https://doi.org/10.3847/1538-4357/ad4a62.
[58] Nidhi, S., Mathew, B., Shridharan, B., Arun, R., Anusha, R., & Kartha, S. S. (2023). Spectroscopic study of Herbig Ae/Be stars in the Galactic anti-centre region from LAMOST DR5. Monthly Notices of the Royal Astronomical Society, 524(4), 5166–5181. https://doi.org/10.1093/mnras/stad2067.
[59] Díaz, R. F., Cincunegui, C., & Mauas, P. J. D. (2007). The Na I D resonance lines in main-sequence late-type stars. Monthly Notices of the Royal Astronomical Society, 378(3), 1007–1018. https://doi.org/10.1111/j.1365-2966.2007.11833.x.
[60] Eiroa, C., Oudmaijer, R. D., Davies, J. K., de Winter, D., Garzón, F., Palacios, J., Alberdi, A., Ferlet, R., Grady, C. A., Cameron, A. C., Deeg, H. J., Harris, A. W., Horne, K. D., & Merín, B. (2002). On the simultaneous optical and near-infrared variability of pre-main sequence stars. Astronomy & Astrophysics, 384, 1038–1049. https://doi.org/10.1051/0004-6361:20020096.
[61] Kesseli, A. Y., Petkova, M. A., Wood, K., Whitney, B. A., Hillenbrand, L. A., Gregory, S. G., Stauffer, J. R., Morales-Calderón, M., Rebull, L., & Alencar, S. H. P. (2016). A Model for (Quasi-) Periodic Multiwavelength Photometric Variability in Young Stellar Objects. The Astrophysical Journal, 828(1), 42. https://doi.org/10.3847/0004-637X/828/1/42.
[62] Akansoy, D., Petrou, H., Ballabio, G., Penzlin, A., (2025). Modelling shadows in scattered light observations as signals from companions in pro-toplanetary discs. Monthly Notices of the Royal Astronomical Society, 540(4), 3186–3203. https://doi.org/10.1093/mnras/staf925.
[63] Ziampras, A., Dullemond, C. P., Birnstiel, T., Benisty, M., & Nelson, R. P. (2025). Spirals, rings, and vortices shaped by shadows in protoplanetary discs: from radiative hydrodynamical simulations to observable signatures. Monthly Notices of the Royal Astronomical Society, 540(1), 1185–1201. https://doi.org/10.1093/mnras/staf785.
[64] Li, R., Chen, Y.-X., & Lin, D. N. C. (2024). Dust accumulation near the magnetospheric truncation of protoplanetary discs – II. The effects of opacity and thermal evolution. Monthly Notices of the Royal Astronomical Society, 529(2), 893–902. https://doi.org/10.1093/mnras/stae581.
[65] Jang, H., Waters, R., Kamp, I., & Dullemond, C. P. (2024). Spatial distribution of crystalline silicates in protoplanetary disks: How to interpret mid-infrared observations. Astronomy & Astrophysics, 687, A275. https://doi.org/10.1051/0004-6361/202348630.
[66] Almeyda, T., Robinson, A., Richmond, M., Vazquez, B., & Nikutta, R. (2017). Modeling the infrared reverberation response of the circumnuclear dusty torus in AGNs: the effects of cloud orientation and anisotropic illumination. The Astrophysical Journal, 843(1), 3. https://doi.org/10.3847/1538-4357/aa7687.
[67] Bensberg, A., & Wolf, S. (2022). Time-dependent Monte Carlo continuum radiative transfer. Astronomy & Astrophysics, 668, A120. https://doi.org/10.1051/0004-6361/202142970.
[68] Lucas, P. W., Smith, L. C., Guo, Z., Contreras Peña, C., Minniti, D., Miller, N., Alonso-García, J., Catelan, M., et al. (2024). The most variable VVV sources: eruptive protostars, dipping giants in the nuclear disc and others. Monthly Notices of the Royal Astronomical Society, 528(2), 1789–1822. https://doi.org/10.1093/mnras/stad3929.
[69] Zsidi, G., Kóspál, Á., Ábrahám, P., Alecian, E., Alencar, S. H. P., Bouvier, J., Hussain, G. A. J., et al. (2025). Short-and long-term variations of the high mass accretion rate classical T Tauri star DR Tau. Astronomy & Astrophysics, 699, A221. https://doi.org/10.1051/0004-6361/202449576.
[70] Herczeg, G. J., Chen, Y., Donati, J.-F., Dupree, A. K., Walter, F. M., Hillenbrand, L. A., Johns-Krull, C. M., et al. (2023). Twenty-five years of accretion onto the classical T Tauri star TW Hya. The Astrophysical Journal, 956(2), 102. https://doi.org/10.3847/1538-4357/acf468.
[71] Kwan, J. (2024). Continuum and line emission from accretion shocks at T Tauri stars – I. Correlations with shock parameters. Monthly Notices of the Royal Astronomical Society, 531(3), 3744–3769. https://doi.org/10.1093/mnras/stae1385.
[72] Kaeufer, T., Min, M., Woitke, P., Kamp, I., & Arabhavi, A. M. (2024). Bayesian analysis of the molecular emission and dust continuum of pro-toplanetary disks. Astronomy & Astrophysics, 687, A209. https://doi.org/10.1051/0004-6361/202449936.
[73] Meldorf, C., Palmese, A., & Salim, S. (2024). Measuring the dust attenuation law of galaxies using photometric data. Monthly Notices of the Royal Astronomical Society, 531(3), 3242–3255. https://doi.org/10.1093/mnras/stae1373.
[74] Gebek, A., Diemer, B., Martorano, M., van der Wel, A., Pantoni, L., Baes, M., Gabrielpillai, A., et al. (2025). The mass-dependent UVJ diagram at cosmic noon: A challenge for galaxy evolution models and dust radiative transfer. Astronomy & Astrophysics, 695, A90. https://doi.org/10.1051/0004-6361/202452768.
[75] Grayling, M., & Popovic, B. (2025). BayeSN and SALT: a comparison of dust inference across SN Ia light-curve models with DES5YR. Monthly Notices of the Royal Astronomical Society, 542(3), 2060–2073. https://doi.org/10.1093/mnras/staf1345.
[76] Guo, Z., Lucas, P. W., Kurtev, R. G., Borissova, J., Elbakyan, V., et al. (2024). Multiwavelength detection of an ongoing FUOr-type outburst on a low-mass YSO. Monthly Notices of the Royal Astronomical Society: Letters, 529(1), L115–L122. https://doi.org/10.1093/mnrasl/slad201.
[77] Tobin, J. J., & Sheehan, P. D. (2024). An Observational View of Structure in Protostellar Systems. Annual Review of Astronomy and Astrophysics, 62, 203–241. https://doi.org/10.1146/annurev-astro-052920-103752 .
[78] Masley, A. T., & Hartmann, L. (2025). Observational signatures of outside-in accretion bursts in embedded protostars. Monthly Notices of the Royal Astronomical Society, 544(4), 3210–3218. https://doi.org/10.1093/mnras/staf1908.
[79] Jheonn, H., Lee, J.-E., Lee, J., Lee, S., Lee, H., et al. (2026). Refined Classification of Young Stellar Objects and Asymptotic Giant Branch Stars by Infrared Magnitudes, Colors, and Time-domain Analysis with Machine Learning. The Astrophysical Journal, 996(2), 136. https://doi.org/10.3847/1538-4357/ae25f2.
[80] Healy, B. F., Coughlin, M. W., Mahabal, A., Laz, T. J. du, Drake, A., Graham, M. J., Hillenbrand, L. A., et al. (2024). The ZTF Source Classification Project. III. A Catalog of Variable Sources. The Astrophysical Journal Supplement Series, 272(1), 14. https://doi.org/10.3847/1538-4365/ad33c6.
[81] Elizabethson, A., Serna, J., García-Varela, A., Hernández, J., & Cabrera-García, J. F. (2023). Machine-learning morphological classification of TESS light curves of T Tauri stars. The Astronomical Journal, 166(5), 189. https://doi.org/10.3847/1538-3881/acf865.
[82] Peng, Y., Ristić, M., Kedia, A., O'Shaughnessy, R., Fontes, C. J., et al. (2024). Kilonova light-curve interpolation with neural networks. Physical Review Research, 6(3), 033078. https://doi.org/10.1103/PhysRevResearch.6.033078.
[83] Dullemond, C. P., Juhász, A., Pohl, A., & others. (2012). RADMC-3D: A multipurpose radiative transfer tool. Astrophysics Source Code Library, ascl:1202.015.
[84] Whitney, B. A., Robitaille, T. P., Bjorkman, J. E., Dong, R., Wolff, M. J., Wood, K., & Honor, J. (2013). Three-dimensional radiation transfer in young stellar objects. The Astrophysical Journal Supplement Series, 207(2), 30. https://doi.org/10.1088/0067-0049/207/2/30.
[85] Pinte, C., Ménard, F., Duchêne, G., & Bastien, P. (2006). Monte Carlo radiative transfer in protoplanetary disks. Astronomy & Astrophysics, 459(3), 797–804. https://doi.org/10.1051/0004-6361:20053275.
[86] Pinte, C., Harries, T. J., Min, M., et al. (2009). Benchmark problems for continuum radiative transfer. Astronomy & Astrophysics, 498, 967–980. https://doi.org/10.1051/0004-6361/200811555.
[87] Woitke, P., Kamp, I., & Thi, W.-F. (2009). Radiation thermo-chemical models of protoplanetary disks. Astronomy & Astrophysics, 501, 383–406. https://doi.org/10.1051/0004-6361/200811467.